Korea-Australia Rheology Journal
Vol. 21, No. 4, December 2009 pp. 245-268

# Micro and macro in the dynamics of dilute polymer solutions: Convergence of theory with experiment

**J. Ravi Prakash***
*Department of Chemical Engineering, Monash University, Melbourne, VIC 3800, Australia*
(Received October 7, 2009; final revision received October 7, 2009)

## Abstract

Recent developments in dilute polymer solution rheology are reviewed, and placed within the context of the general goals of predicting the complex flow of complex fluids. In particular, the interplay between the use of polymer kinetic theory and continuum mechanics to advance the microscopic and the macroscopic description, respectively, of dilute polymer solution rheology is delineated. The insight that can be gained into the origins of the high Weissenberg number problem through an analysis of the configurational changes undergone by a single molecule at various locations in the flow domain is discussed in the context of flow around a cylinder confined between flat plates. The significant role played by hydrodynamic interactions as the source of much of the richness of the observed rheological behaviour of dilute polymer solutions is highlighted, and the methods by which this phenomenon can be incorporated into a macroscopic description through the use of closure approximations and multiscale simulations is discussed.

***Keywords*** **:** dilute polymer solutions, polymer kinetic theory, continuum mechanics, hydrodynamic interactions, high Weissenberg number problem, Brownian dynamics simulation, closure approximations

## 1. Introduction

There have been a number of developments in the last decade or so that have led to significant progress in our capacity to describe the complex flow of dilute polymer solutions. These advances have occurred both through improvements in molecular models developed with polymer kinetic theory, and through the development of sophisticated numerical algorithms for continuum level descriptions. In this paper, I will review some of these developments, and attempt to place them within the context of the general framework that underpins the rheological description of any complex fluid. Though there have been many important contributors to these developments (see for instance Larson (2004) and Shaqfeh (2005) for recent reviews), and their work is no sense less significant, this review will largely use the work done by the rheology group at Monash university as the basis for the arguments that form the main contention of this paper, namely, that a fairly clear idea has emerged in recent years on where the future direction of rheology research on dilute polymer solutions should be focussed.

The schematic diagram in Fig. 1 is an attempt to visualize the different aspects that combine together to form what might be called "complex fluid mechanics". Similar diagrams have been used before for this purpose (Boger, 1996), and they wonderfully capture the essence of the enterprise that complex fluid mechanicians are generally embarked upon. This diagram will be referred to frequently in the paper, and provides the context for all the discussions in it.

The diagram has two parts to it, a macroscopic cycle and a microscopic cycle. The macroscopic cycle begins with conservation laws of continuum mechanics such as the balances of mass, momentum and energy, augmented with an appropriate constitutive equation. For instance, as is well known, a constitutive equation that describes the behaviour of dilute polymer solutions is the Oldroyd-B model. These equations, with appropriate boundary conditions, are solved using a numerical technique such as the finite element method (FEM), to compute both the velocity and stress fields in the complex geometry that is of interest, arising from the flow of the complex fluid. The predictions of these fields are then compared with experimental observations. If the comparison is not satisfactory, phenomenological theories are used to improve the constitutive equation, which is essentially a repository of information about the particular complex fluid that is of interest. This cycle is repeated until convergence is obtained (by which is meant that there is agreement between theory and experiment).

*Corresponding author: ravi.jagadeeshan@eng.monash.edu.au

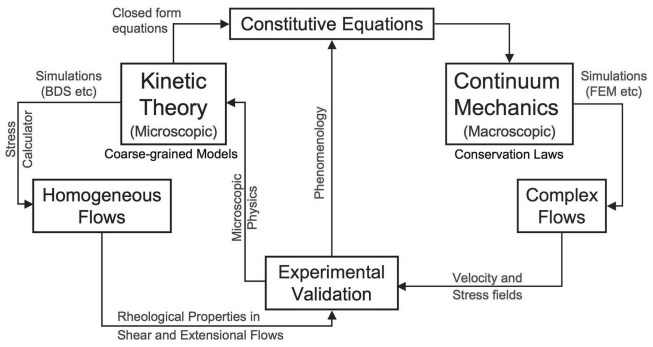


**Fig. 1.** Schematic diagram describing the macroscopic and microscopic approaches to complex fluid mechanics.

In the microscopic cycle, one begins with the equations of kinetic theory that describe the time evolution of the configurations of the microstructure of the complex fluid. The microstructure is usually represented by some coarse-grained model. For instance, polymer molecules are frequently represented by bead-spring chains. The motion in time of the microstructure is computed with a mesoscopic simulation algorithm, of which, depending on the level of coarse-graining, there are currently a wide variety to choose from, such as molecular dynamics, Brownian dynamics, dissipative particle dynamics etc. With the help of an equation that relates the instantaneous configurations of the microstructure to the stress in the fluid (such as Kramers expression for dilute polymer solutions), rheological properties in homogeneous flows such as simple shear or extensional flows can be obtained. In general, derivations of configurational time evolution equations in kinetic theory are restricted to homogeneous flows. A comparison is then made between predictions and experimental observations. If one doesn't have agreement, additional physics at the microscopic scale are included and the cycle is repeated until convergence is obtained.

As is well known, kinetic theory can also be used to derive closed form constitutive equations which can then be used within the context of continuum mechanics to carry out the macroscopic cycle.

The aim of this paper is to use the schematic representation in Fig. 1 to place recent work on dilute polymer solutions in perspective. In particular, the argument will be made that while significant progress has been made in achieving convergence in the microscopic cycle, there is still quite a long way to go before convergence in the macroscopic cycle can be achieved. As mentioned earlier, this review is not exhaustive, and only aims to give a flavour of the issues involved, heavily coloured by the set of problems that have been pursued in our group. Attention is restricted to discussing the behaviour of flexible linear polymer molecules in $\theta$-solutions, and none of the important problems that arise in the context of polyelectrolyte solutions, branched polymers, semi-flexible/rigid polymers etc are discussed.

## 2. The Macroscopic Cycle

We first consider the macroscopic cycle for a dilute polymer solution. As is well known, the simplest constitutive equation which is capable of capturing some of the observed features of a polymer solution (such as a non-zero first normal stress difference) is the Oldroyd-B model. The Oldroyd-B model assumes that the total stress is a sum of the solvent and polymer contributions to stress, with the solvent stress $\boldsymbol{\tau}_s$ given by Newtons law of viscosity, and the polymer contribution $\boldsymbol{\tau}_p$ given by the upper convected Maxwell model,

$$\boldsymbol{\sigma} = \boldsymbol{\tau}_s + \boldsymbol{\tau}_p \tag{1}$$

$$\boldsymbol{\tau}_s = -2\eta_s \mathbf{D} \tag{2}$$

$$\boldsymbol{\tau}_p + \lambda\left(\frac{\partial \boldsymbol{\tau}_p}{\partial t} + \mathbf{v}\cdot\nabla\boldsymbol{\tau}_p - \boldsymbol{\kappa}\cdot\boldsymbol{\tau}_p - \boldsymbol{\tau}_p\cdot\boldsymbol{\kappa}^T\right) = -2\eta_p\mathbf{D} \tag{3}$$

where, $\eta_s$ is the solvent viscosity, $\eta_p$ is the polymer contribution to viscosity, $\lambda$ is the polymer relaxation time, $\boldsymbol{\kappa} = \nabla \mathbf{v}^T$ is the transpose of the velocity gradient, and $\mathbf{D} = 1/2(\boldsymbol{\kappa} + \boldsymbol{\kappa}^T)$ is the rate of deformation tensor. When written in non-dimensional form (with the velocity gradient non-dimensionalised by $\dot{\gamma} = \sqrt{\mathbf{D}:\mathbf{D}}$, which is the second invariant of $\mathbf{D}$, and stress by $\eta\dot{\gamma}$, where $\eta = \eta_s + \eta_p$ is the solution viscosity), these equations become,

$$\boldsymbol{\sigma} = \boldsymbol{\tau}_s + \boldsymbol{\tau}_p \tag{4}$$

$$\boldsymbol{\tau}_s = -2\beta\mathbf{D} \tag{5}$$

$$\boldsymbol{\tau}_p + Wi\left(\frac{\partial \boldsymbol{\tau}_p}{\partial t} + v\cdot\nabla\boldsymbol{\tau}_p - \boldsymbol{\kappa}\cdot\boldsymbol{\tau}_p - \boldsymbol{\tau}_p\cdot\boldsymbol{\kappa}^T\right) + 2(1-\beta)\mathbf{D} = 0 \tag{6}$$

Clearly, two non-dimensional parameters arise that characterize the fluid and the flow. The first being the viscosity ratio $\beta = \eta_s/\eta$, and the second the Weissenberg number $Wi = \lambda\dot{\gamma}$.

When combined with the conservation of mass and

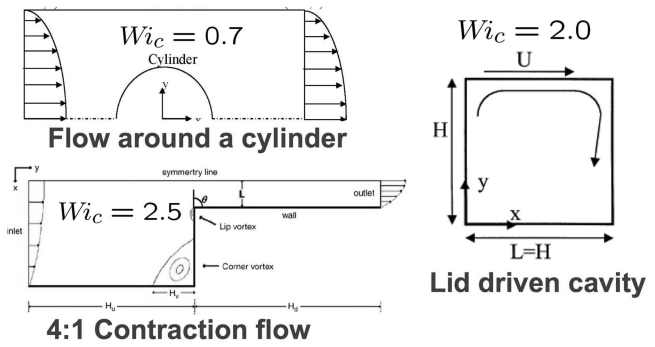


**Fig. 2.** Representative benchmarks flows, with the typical critical Weissenberg number at which breakdown of computations occurs indicated as $Wi_c$.

momentum, these equations have been solved numerically and analytically over the years in a variety of situations. Unfortunately, however, in most geometries, numerical computations break down as the Weissenberg number increases beyond a threshold value.

This problem, known as the high Weissenberg number problem (HWNP), occurs due to the development of very large stresses and stress gradients in narrow regions of the flow field, and the challenge of overcoming this problem has been the driving force behind the development of a wide range of advanced numerical techniques (Keunings, 2000; Owens and Phillips, 2002). In spite of these advances, computations disappointingly still break down at Weissenberg numbers of $O(1)$, and it is still not clear whether this is because solutions do not exist at higher values of $Wi$, or whether it is simply due to the inadequacy of current numerical techniques (Keunings, 2000). As a result, one does not yet have the capability of routinely computing viscoelastic flows. In fact, rather than compute complex flows, the non-Newtonian fluid mechanics community has focussed its attention on first solving benchmark problems, typical examples of which are indicated in Fig. 2. The basic idea is that once the origin of the HWNP is understood and tamed in well characterized geometries, then more difficult situations involving complex flows of industrial relevance can be tackled. It is perhaps fair to say, consequently, that far from having convergence between theory and experiment, one is still in the stage of computing velocity and stress fields reliably.

## 3. The Microscopic Cycle

We now consider the microscopic cycle and trace the developments that have occurred in describing dilute polymer solutions at a microscopic scale. Unlike simple Newtonian fluids, it becomes essential to consider the role of the microstructure in complex fluids since the microstructure significantly influences macroscopic properties and is in turn affected by it. Fortunately, for many of the properties one is interested in, it is not necessary to account for details at the atomistic scale. Since large scale properties, like rheological properties, only depend on general features of polymer molecules such as the fact that they can be stretched, oriented and have many degrees of freedom, it is sufficient quite often to use coarse-grained models to describe a polymer chain. Further, since the solvent molecules are much smaller than polymer molecules, and their motion occurs over much smaller time scales, the solvent is frequently neglected altogether, and replaced by its net effect on the polymer molecule. For instance, it is considered to be the seat of a Brownian force and a drag force that act on the polymer molecule.

As is well known, the most accurate coarse-grained model for a finite flexible polymer molecule is the bead-rod model, with as many rods as there are Kuhn steps $N_k$ in the polymer chain (Bird *et al*., 1987b). While using a bead-rod model for the polymer chain in mesoscopic simulations is indeed feasible for short chains (with $N_k \lesssim 200$), unfortunately, this is not the case for the typical polymer molecular weights commonly encountered in practice. For instance, a polystyrene molecule of 2 million molecular weight has roughly 2600 Kuhn steps (Prabhakar *et al.*, 2004). A coarse-grained model with such a large number of degrees of freedom is still far beyond current computational capacity. An alternative approach is to use a more coarse-grained model such as a bead-spring chain with $N$ beads, with $N << N_k$, where each spring represents $N_k/(N-1)$ Kuhn steps. The limit of this approach is the Hookean dumbbell model, indicated in Fig. 3, which represents the entire chain with just one degree of freedom, the end-to-end vector $\mathbf{Q}$.

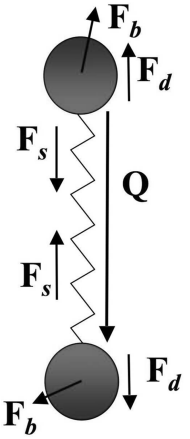


**Fig. 3.** The dumbbell model for a polymer molecule in a dilute solution, with a schematic indication of the various forces acting on the beads.

In the presence of a flow field, with inertia neglected, a balance of the hydrodynamic drag force $\mathbf{F}_d$, the Brownian force $\mathbf{F}_b$, and the spring force $\mathbf{F}_s$ on a bead, leads to the following equation of motion for the connector vector $\boldsymbol{Q}$ between the beads,

$$\mathbf{0} = -\zeta(\dot{\boldsymbol{Q}} - \boldsymbol{\kappa}\cdot\boldsymbol{Q}) - 2k_B T\frac{\partial}{\partial \boldsymbol{Q}}\ln\psi - 2\mathbf{F}_c \tag{7}$$

where, $\zeta$ is the Stokesian bead-friction coefficient (which is related to the bead radius $a$ through $\zeta = 6\pi a\eta_s$), $k_B$ is the Boltzmann constant, $T$ is the temperature, the term containing the logarithm of the configurational distribution function $\psi(\boldsymbol{Q})$ represents the Brownian force, and $\mathbf{F}_c$ is the "connector" force between the beads (which is equal to $\mathbf{F}_s$ in the direction of $\boldsymbol{Q}$) (Bird *et al*., 1987b). Note that $\boldsymbol{\kappa}$ here is the transpose of the velocity gradient in a *homogeneous* flow field. When the equation of motion is combined with the equation of continuity for the distribution function $\psi$, the following *diffusion* equation for $\psi$ is obtained (Bird *et*

*al*., 1987b),

$$\frac{\partial \psi}{\partial t} = -\left( \frac{\partial}{\partial \boldsymbol{Q}} \cdot \left\{ [\boldsymbol{\kappa} \cdot \boldsymbol{Q}] \psi - \frac{2k_B T}{\zeta} \frac{\partial \psi}{\partial \boldsymbol{Q}} - \frac{2}{\zeta} \mathbf{F}_c \psi \right\} \right) \tag{8}$$

which describes the time evolution of the probability distribution for finding a dumbbell with internal configuration in the range $d\boldsymbol{Q}$ about $\boldsymbol{Q}$.

The stress contribution due to the presence of the polymer can be calculated by an expression that relates the stress to the configuration of the molecules. In the case of a dumbbell model, this is the well known Kramers expression (Bird *et al*., 1987b),

$$\boldsymbol{\tau}_p = -n_p \langle \boldsymbol{Q} \mathbf{F}_c \rangle + n_p k_B T \boldsymbol{\delta} \tag{9}$$

where, $n_p$ is the number density of polymer molecules, the angular brackets represent an ensemble average over the distribution function $\psi$, and $\boldsymbol{\delta}$ is the identity tensor. For Hookean dumbbells, since $\mathbf{F}_c = H\boldsymbol{Q}$, with $H$ being the spring constant of the Hookean spring in the dumbbell, the Kramers expression is,

$$\boldsymbol{\tau}_p = -n_p H \tilde{\mathbf{M}} + n_p k_B T \boldsymbol{\delta} \tag{10}$$

where, the quantity $\tilde{\mathbf{M}} = \langle \boldsymbol{QQ} \rangle$ is the second moment of the end-to-end vector $\boldsymbol{Q}$, commonly also referred to as the conformation tensor in continuum mechanics literature. The eigenvalues and eigenvectors of $\tilde{\mathbf{M}}$ provide insight into the mean stretch and orientation of the polymer molecules. Clearly, if the second moment can be evaluated, then all the rheological properties in any flow field can be determined.

A time evolution equation for the conformation tensor can be derived by multiplying Eq. (8) by the dyadic product $\boldsymbol{QQ}$ and integrating over all configurations of the dumbbell,

$$\frac{\partial \tilde{\mathbf{M}}}{\partial t} + \boldsymbol{v} \cdot \nabla \tilde{\mathbf{M}} - \boldsymbol{\kappa} \cdot \tilde{\mathbf{M}} - \tilde{\mathbf{M}} \cdot \boldsymbol{\kappa}^T = -\frac{1}{\lambda_H} \left[ \tilde{\mathbf{M}} - \frac{k_B T}{H} \mathbf{I} \right] \tag{11}$$

where, $\lambda_H = \zeta/4H$ is the usual dumbbell relaxation time.

The connection between the microscopic and macroscopic cycle can now be derived in a straightforward manner. By eliminating the conformation tensor $\tilde{\mathbf{M}}$ from the time evolution equation (11) using Kramers expression (Eq. (10)), and making the following mappings between microscopic and macroscopic variables: $\lambda_H = \lambda$ and $n_p k_B T \lambda_H = \eta_p$, one gets back the Oldroyd-B model (Eq. (3)) of continuum mechanics. This suggests that essentially the Hookean dumbbell model and the Oldroyd-B model are two different representations of the same physics, and whatever insight ones derives from the Hookean dumbbell model can be applied to understanding results of using the Oldroyd-B model.

Notice that the conformation tensor $\tilde{\mathbf{M}}$ appears on the left-hand-side and the righthand-side of the time evolution equation (11). This makes it possible, as we have just done, to eliminate $\tilde{\mathbf{M}}$ using Kramers expression and to replace it with $\boldsymbol{\tau}_p$ instead. In more complicated models in which nonlinear microscopic phenomenon such as finite extensibility or hydrodynamic interactions are incorporated, however, the right-hand-side usually has more complex moments of $\boldsymbol{Q}$. As a result, a closed form equation for $\boldsymbol{\tau}_p$ cannot be derived. This is origin of the need for "closure approximations", which will be discussed in greater detail shortly.

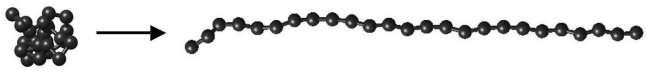

**Fig. 4.** Schematic representation of a polymer molecule undergoing a coil-stretch transition.

As mentioned earlier, once the expression for $\boldsymbol{\tau}_p$ is obtained, predictions in homogeneous flows such as shear flow and extensional flow can be obtained. In a shear flow, as is well known, a polymer solution exhibits shear thinning behaviour, with the viscosity decreasing as a function of shear rate (Bird *et al.*, 1987a). Unfortunately, the Hookean dumbbell model does not predict shear thinning (Bird *et al*., 1987b).

The model performs even more poorly in uniaxial extensional flows. At a critical value of Weissenberg number $Wi = 0.5$, the extensional viscosity is predicted to be unbounded (Bird *et al*., 1987b). Since it is possible to track the magnitude of the end-to-end vector at the same time, it can be shown that this occurs because, precisely at $Wi = 0.5$, the dumbbell undergoes a sharp coil-stretch transition and stretches indefinitely (as illustrated schematically in Fig. 4). The problem is clearly due to the infinite extensibility of the Hookean spring in the model.

This is the point at which the iterative process in the microscopic cycle begins. Since one has failed to obtain a sensible macroscopic prediction, there is a need to improve the physical representation of the reality at the microscopic scale. The most obvious solution is to make the molecules' length finite, which would make more realistic the coarse-grained representation of the polymer molecule. As mentioned earlier, using a bead-rod model, which would accurately model the polymer molecules finiteness, is not a practical option currently. A simpler solution is to use a nonlinear spring in place of the Hookean spring, i.e., a spring that becomes increasing difficult to stretch as the maximum allowed stretch of the spring is approached. Each spring in a finitely extensible bead-spring chain model would have a maximum stretchable length $Q_0$, such that, $Q_0 = N_k b_k/(N-1)$, where $b_k$ is the length of an individual Kuhn step. The simplest model in this case would be a dumbbell with a single finitely extensible spring. Different spring force laws have been suggested in the literature, such as the Finitely Extensible Nonlinear Elastic (FENE) force law (Warner, 1972) or the Worm-like-chain (WLC)

force law (Marko and Siggia, 1995), which reflect the different extents of flexibility of the chain.

With the use of a finitely extensible bead-spring chain model, the problem of unbounded extensional viscosity disappears. A simple demonstration of this result in the context of a dumbbell model, where asymptotic results at small and large extension rates can be derived analytically, can be found in the textbook by Bird *et al.* (1987b). The polymer still undergoes a coil-stretch transition at $Wi = 0.5$, but the viscosity remains bounded as the spring approaches its fully stretched value. Interestingly, as the extensibility of the spring becomes large, the finitely extensible spring approaches a Hookean spring, and the extensional viscosity again becomes unbounded.

Since the expression for the connector force in a finitely extensible spring is nonlinear, it is not possible to obtain a closed form expression for the stress tensor. Under these circumstances, it turns out there are two approaches that can be adopted in order to evaluate the ensemble average $\langle \boldsymbol{Q}\mathbf{F}_c \rangle$ in Kramers expression (9) at arbitrary values of the extension rate (and not just at the asymptotic limits). The first approach, which leads to an exact (albeit numerical) evaluation of the average, consists of two steps. The first step is to write a stochastic differential equation for the connector vector $\boldsymbol{Q}$, which is equivalent to the diffusion equation (8) (Öttinger, 1996). The second step is to use Brownian dynamics (BD) simulations to integrate the stochastic differential equation in order to obtain an ensemble of stochastic trajectories for $\boldsymbol{Q}$. The average of any quantity that is a function of $\boldsymbol{Q}$ can then be evaluated by carrying out an ensemble average over all these trajectories.

An alternative approach to using BD simulations (which can be computationally intensive), is to implement a closure scheme that enables an evaluation of $\langle \boldsymbol{Q}\mathbf{F}_c \rangle$. Though this method leads to an approximate value of the average, it has the advantage that it leads to a closed form constitutive equation for $\boldsymbol{\tau}_p$ that can then be used in the continuum mechanics context of the macroscopic cycle.

Consider for example the FENE spring. In this case, the connector force is given by the expression,

$$\mathbf{F}_c = \frac{H}{(1-Q^2/Q_0^2)}\boldsymbol{Q} \tag{12}$$

Adopting the first of the above mentioned approaches, the stochastic differential equation that is equivalent to the diffusion equation (8) can be written,

$$d\boldsymbol{Q} = \left[\boldsymbol{\kappa}\cdot\boldsymbol{Q} - \frac{2}{\zeta}\mathbf{F}_c\right]dt + 2\sqrt{\frac{k_BT}{\zeta}}d\mathbf{W} \tag{13}$$

where, $\mathbf{W}$ is a three-dimensional Wiener process. This equation can be integrated numerically with the help of BD simulations to generate an ensemble of trajectories of $\boldsymbol{Q}$. The term $\langle \boldsymbol{Q}\mathbf{F}_c \rangle$ in Kramers expression can then be evaluated as an average over these trajectories, and an exact (numerical) prediction of all rheological properties can be obtained (Öttinger, 1996; Prabhakar and Prakash, 2002a).

An example of the alternative closure approximation approach is the commonly used FENE-P closure, which consists of replacing $Q^2$ in Eq. (12) with its average value (Bird *et al*., 1980),

$$\mathbf{F}_c = \frac{H}{(1-\langle Q^2\rangle/Q_0^2)}\boldsymbol{Q} \tag{14}$$

Once again, by multiplying Eq. (8) by the dyadic product $\boldsymbol{QQ}$ and integrating over all configurations of the FENE-P dumbbell, the following closed expression for the conformation tensor can be derived,

$$\frac{\partial\tilde{\mathbf{M}}}{\partial t} + \boldsymbol{v}\cdot\nabla\tilde{\mathbf{M}} - \boldsymbol{\kappa}\cdot\tilde{\mathbf{M}} - \tilde{\mathbf{M}}\cdot\boldsymbol{\kappa}^T = -\frac{1}{\lambda_H}\left[f(\mathrm{tr}\tilde{\mathbf{M}})\tilde{\mathbf{M}} - \frac{k_BT}{H}\mathbf{I}\right] \tag{15}$$

where, the function $f(\mathrm{tr}\tilde{\mathbf{M}})$ is (Pasquali and Scriven, 2004),

$$f(\mathrm{tr}\tilde{\mathbf{M}}) = \frac{b_M - 1}{b_M - (\mathrm{tr}\tilde{\mathbf{M}}/\mathrm{tr}\tilde{\mathbf{M}}_{eq})} \tag{16}$$

with, $b_M$ representing the *finite extensibility* parameter, defined as $b_M = Q_0^2/\langle Q^2\rangle_{eq}$, and

$$\mathrm{tr}\tilde{\mathbf{M}}_{eq} = \langle Q^2\rangle_{eq} = \frac{3Q_0^2(k_BT/H)}{Q_0^2 + 3(k_BT/H)} \tag{17}$$

Note that the subscript 'Eq' represents a quantity evaluated at equilibrium.

In this case, Kramers expression for the polymer contribution to the total stress is given by,

$$\boldsymbol{\tau}_p = -n_pHf(\mathrm{tr}\tilde{\mathbf{M}})\tilde{\mathbf{M}} + n_pk_BT\boldsymbol{\delta} \tag{18}$$

Together, Eqs. (15) and (18), make up the FENE-P constitutive model. The FENE-P model can be combined with the conservation laws of mass and momentum to lead to a more refined macroscopic model than the Oldroyd-B model, since it captures the finite extensibility of a polymer molecule. This model is discussed subsequently when we revisit the macroscopic cycle in section 4. Here, we discuss the implications of the introduction of the FENE spring in place of the Hookean spring.

Since physically meaningful values of the extensional viscosity can be predicted with a bead-spring chain with finitely extensible springs, it becomes possible to compare theoretical predictions with experimental measurements of the extensional viscosity. Before discussing such a comparison however, it is worth making a few observations about the experimental determination of the extensional viscosity.

The accurate measurement of the extensional viscosity of a polymeric fluid has been a significant challenge for experimental rheologists because of the difficulty in generating a pure uniaxial extensional flow. A final resolution of this problem was only attained in the early 1990s through the development of the Filament Stretching Rhe-

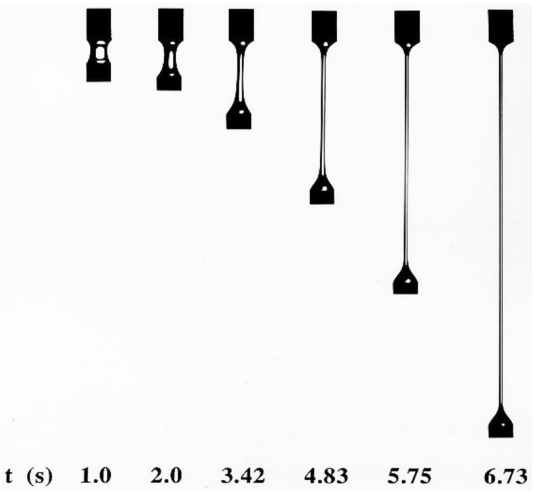


**Fig. 5.** Snapshots of a filament at various times as it is being extended in a Filament Stretching Rheometer.

ometer (FISER) in Sridhar's laboratory at Monash University (Tirtaatmadja and Sridhar, 1993). As demonstrated by the snapshots of a stretching filament of fluid in Fig. 5, a sample of fluid is stretched exponentially in the FISER in the vertical direction. The change in the mid-filament diameter is measured with a laser, while simultaneously the forces in the filament are measured with force transducers at the end plates. The FISER procedure has been standardized to remove various non-idealities in the flow kinematics and provides the most reliable measurement of the elongational stress as a function of strain rate that is currently available, and has proved to be a very robust method for the measurement of the extensional viscosities of a wide array of complex fluids (McKinley and Sridhar, 2002).

The first attempt to make a direct comparison between predictions of Brownian dynamics simulations and experimental measurements in Sridhar's laboratory of the extensional viscosity of a dilute polymer solution, in the context of a bead-spring chain model with finitely extensible springs, was by Li *et al.* (2000). Fig. 6 displays the results of their comparison for the Trouton ratio (which is a ratio of the extensional viscosity to the zero shear rate viscosity) as a function of time, observed during the extensional flow of 1.95 million molecular-weight polystyrene solutions. Clearly the simulations capture remarkably accurately all the qualitative features of the growth in the Trouton ratio with time, and even do a reasonable job of obtaining quantitative agreement. However, the discrepancy that can still be observed between experiment and theory suggests that including finite extensibility alone is perhaps not sufficient to achieve convergence of theory with experiment. As will be discussed in greater detail when we return to the microscopic cycle in section 5, it turns out that there are a number of aspects of the simulations that can be improved upon. For instance, one can make a more rational choice of

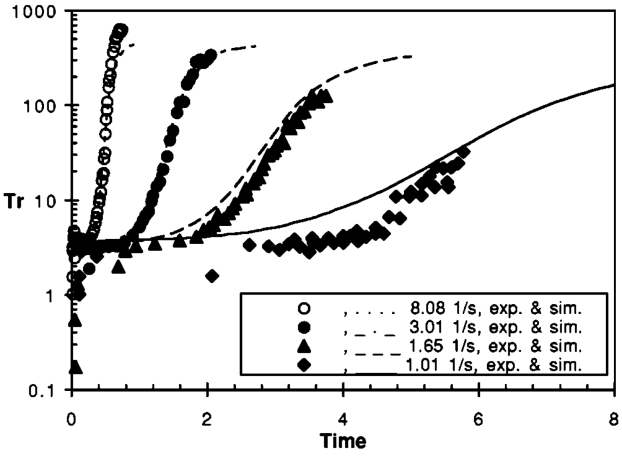


**Fig. 6.** Comparison between simulation (lines) and the experimental results (symbols) for the Trouton ratio versus time of 1.95 million molecular-weight polystyrene solutions undergoing uniaxial extensional flow at various extension rates. Reprinted figure with permission from L. Li, R. G. Larson, and T. Sridhar, Journal of Rheology, 44, 291-322, 2000. (http://dx.doi.org/10.1122/1.551087) Copyright 2009 by the American Physical Society.

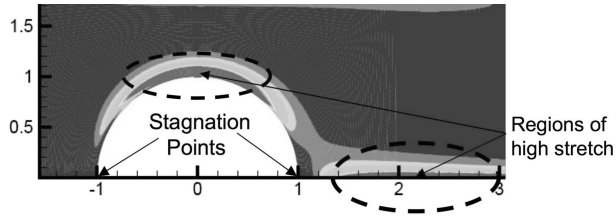


**Fig. 7.** Schematic representation of regions of high polymer stretch along the boundary and in the wake of a cylinder arising from the flow of a viscoelastic fluid around it.

the parameters used in the simulations. More importantly, recent experimental observations of coil-stretch hysteresis in dilute polymer solutions have made it clear that it is crucial to incorporate the nonlinear phenomenon of hydrodynamic interactions into the theoretical description before an adequate description of polymer solution rheology can be obtained. Before exploring these developments, however, it is appropriate to first discuss developments in the macroscopic cycle that mirrored the microscopic recognition of the importance of incorporating the finite extensibility of the polymer molecule.

## 4. The Macroscopic Cycle Revisited

Nearly two decades ago, Rallison and Hinch (1988) argued in a seminal paper that in the case of the Oldroyd-B model, the inability to compute macroscopic flows at highWeissenberg numbers has a physical origin in the infinite extensibility of the Hookean spring that underlies the model. By considering the simple example of a stagnation point flow

of an Oldroyd-B fluid, they showed that when the strain rate is supercritical, infinite stresses can occur in the interior of a steady flow, brought about by the unbounded stretching of polymer molecules. Based on their analysis, they suggested the use of a constitutive equation that is derived from a microscopic model with a nonlinear spring force law as an obvious remedy for the HWNP.

Chilcott and Rallison (1988) examined the benchmark complex flow problems of unbounded flow around a cylinder and a sphere, using a dumbbell model with finite extensibility, as a means of demonstrating the validity of this analysis. In order to understand the coupling between the polymer extension by flow, the stresses developed in the fluid, and the resultant flow field, they deliberately used the conformation tensor as the fundamental variable instead of the stress, and used kinetic theory to derive a simple closed from expression relating the conformation tensor to the polymer contribution to the stress. This constitutive model is now referred to as the FENE-CR model. By solving the equation for the conformation tensor along with the mass and momentum conservation laws, Chilcott and Rallison showed that even though there existed highly extended material close to the boundary and in the wake of a cylinder (as indicated schematically in Fig. 7), there no longer was an upper limit to *Wi* in the range of values accessible in their computations. Because the degree of molecular extension is directly related to the magnitude of stress, the Chilcott and Rallison procedure established a clear connection between high stresses and stress gradients in the flow domain with the configurational and spatial distribution of polymer conformations. Indeed, when simulations were carried out with the polymer length set to infinity rather than a finite value, the downstream structure could not be resolved, and the mean stretch of the polymers in the flow direction continued to grow with increasing *Wi* until the solution failed.

Despite this compelling demonstration of the physical origin of the HWNP, the Oldroyd-B model continues to be used extensively in computational rheology. There are perhaps at least two reasons for this. Firstly, there is a feeling that in a complex flow, the velocity field will adapt itself to avoid the stress becoming singular through some kind of "self-correction" mechanism. Secondly, even if the stresses are large, since they are not infinite it might be possible to develop robust numerical algorithms that finally overcome the HWNP problem. In support of this argument, Wapperom and Renardy (2005) considered the case of an *ultradilute* solution where the velocity field is decoupled from the polymer stress and showed that solutions exist for arbitrarily large Weissenberg numbers. Until very recenty, there has been no conclusive demonstration that bounded solutions for the viscoelastic stress do not exist in complex flows at high values of *Wi*. However, several papers have appeared in the past few years showing analytically that in the special case of steady flows with an interior stagnation point, or in steady stagnation point flows away from a wall, the mathematical structure of the upper convected Maxwell, Oldroyd-B and FENE-P models can be expected to lead to singularities in the viscoelastic stresses and their gradients with increasing *Wi* (Becherer *et al.*, 2008, 2009; Renardy, 2006).

The use of the conformation tensor as the fundamental quantity rather than the stress has become common in computational rheology, and the challenge of developing numerical methods capable of resolving steep stresses and stress gradients has been transformed to one of developing techniques capable of resolving rapidly varying conformation tensor fields. In an important recent breakthrough, Fattal and Kupferman (2004) have shown that by changing the fundamental variable to the matrix logarithm of the conformation tensor, stable numerical solutions can be obtained at values of *Wi* significantly greater than ever obtained before. They argue that the need for this variable transformation arises due to the inability of conventional

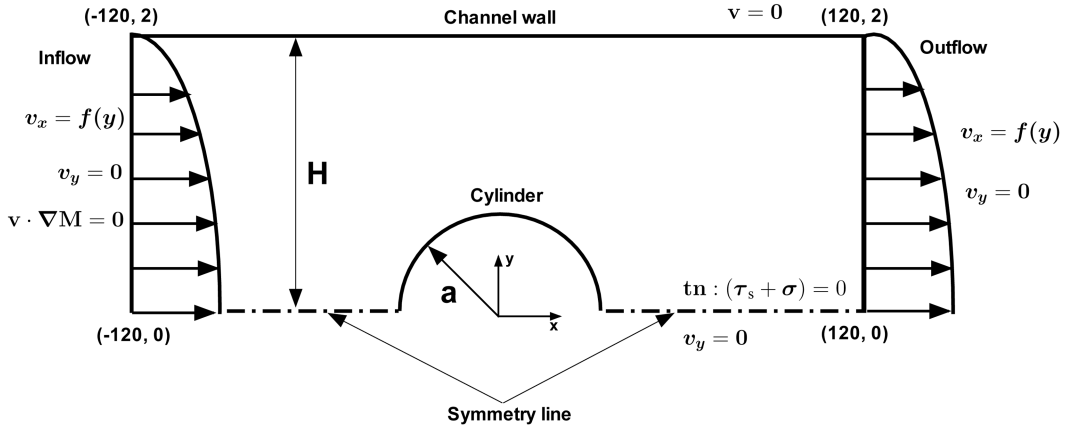


**Fig. 8.** Flow around a cylinder confined between two flat plates. Boundary conditions at the various boundaries are indicated. Reprinted figure with permission from M. M. Bajaj, M. Pasquali and J. R. Prakash, Journal of Rheology 52, 197-223, 2008. (http://dx.doi.org/10.1122/1.2807444) Copyright 2009 by the American Physical Society.

methods based on polynomial basis functions to adequately represent the exponential profiles that emerge in conformational tensor fields in the vicinity of stagnation points and in regions of high deformation rate. Hulsen *et al.* (2005) have recently carried out a stringent test of the log conformation representation by examining the flow of an Oldroyd-B fluid around a cylinder confined between parallel plates. A schematic of this geometry is depicted in Fig. 8. They found that with the log conformation formulation, the solution remains numerically stable for values of *Wi* considerably greater than those obtained previously with standard FEM implementations. However, with regard to the behavior of the convergence of the solution with mesh refinement, they found that the log conformation formulation fails to achieve mesh convergence in the entire wake region at roughly the same value ($Wi \gtrsim 0.6$) as in previous studies. Thus, the HWNP still persists with the Oldroyd-B model, and until recently its origin remained a mystery.

In a recent paper, however, Bajaj *et al.* (2008) have conclusively established the connection between the HWNP and the unphysical behavior of the Oldroyd-B model, in the benchmark problem of the steady symmetric two-dimensional flow around a cylinder confined between parallel plates. Basically, insight into the HWNP has been gained by considering: (i) the behaviour of a packet of fluid containing an ensemble of dumbbells starting close to the downstream stagnation point and travelling along the the symmetry line in the wake of the cylinder, and (ii) the implications of the form of the conformation tensor equation along the symmetry line.

Using the Newtonian velocity field computed by FEM, Bajaj *et al.* (2008) have shown that material particles travelling down the centreline in the cylinder wake accumulate a significant amount of strain (of roughly eight Hencky units) due to the extended period of time that they spend in the neighbourhood of the stagnation point. The behavior of individual molecules in an ultra-dilute solution as they are subjected to this degree of straining, was also examined. Basically, trajectories of Hookean dumbbells convected by the flow field down the centerline, subjected to the local strain rate, were computed using BD simulations. Nearly all the dumbbells in the ensemble were found to be close to their initial state of extension until approximately five strain units, beyond which several of the dumbbells were seen to undergo rapid extension (which is a clear signature of a *coil-stretch* transition), with the extension becoming more pronounced as the *Wi* increased. Very recently, François *et al.* (2008) have examined the flow around a cylinder of PEO polymer solutions seeded with a small amount of fluorescently labeled DNA molecules and have obtained graphic visual images of the presence of narrow regions of highly stretched DNA molecules in the vicinity of a cylinder, which they propose implies the existence of a coil-stretch transition.

The lack of convergence with mesh refinement for the Oldroyd-B model is usually seen most drastically in the failure of different meshes to yield a converged value of the maximum that occurs in the polymeric stress component $\tau_{p,xx}$ on the centerline in the wake of the cylinder. As will be discussed in greater detail shortly, the results of Bajaj *et al.* (2008) clearly indicate that this failure is linked to the polymer molecules undergoing a coil-stretch transition in the wake of the cylinder, since the coil-stretch

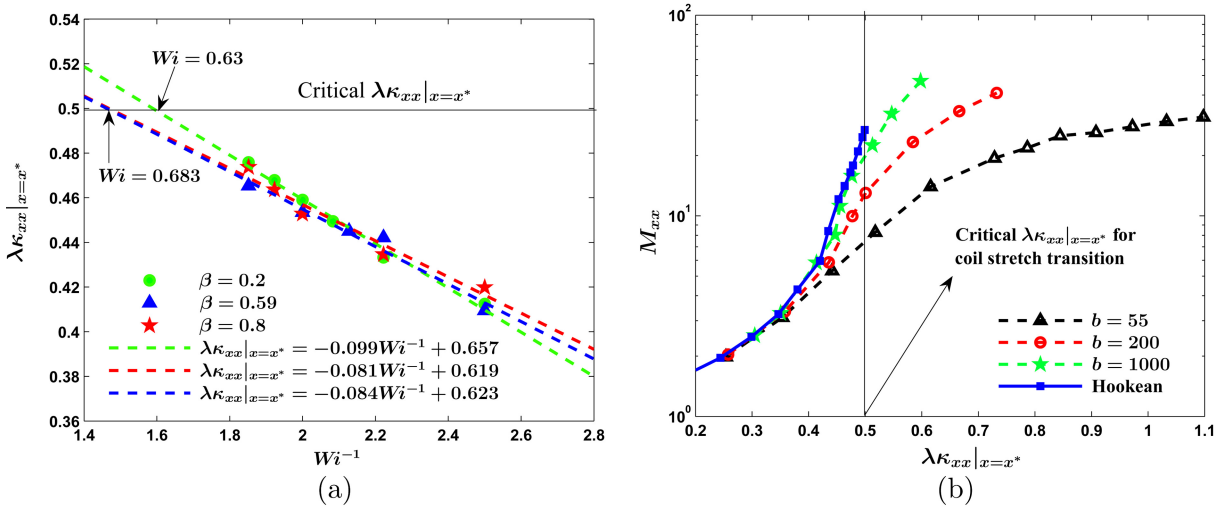


**Fig. 9.** (a) Dependence of the non-dimensional strain rate $\lambda\kappa_{xx}$ on $Wi^{-1}$, at the location $x = x^*$ of the maximum in $M_{xx}$ in the cylinder wake, for a dilute Oldroyd-B fluid. (b) Variation of the polymer stretch $M_{xx}$ at the location of the stress maxima with $\lambda\kappa_{xx}|_{x=x^*}$, for Oldroyd-B and FENE-P models for the viscosity ratio $\beta = 0.59$. Reprinted figure with permission from M. M. Bajaj, M. Pasquali and J. R. Prakash, Journal of Rheology 52, 197-223, 2008. (http://dx.doi.org/10.1122/1.2807444) Copyright 2009 by the American Physical Society.

transition is found to occur in the vicinity of the location of the maximum in the normal stress component.

Interestingly, when Bajaj *et al.* (2008) compared the magnitude of the dumbbells to the length of an element in the finite element mesh, they found that some of the molecules were large enough to span several elements. The possibility that under certain circumstances polymer length scales can become comparable to the mesh size in finite element simulations was anticipated several years ago by Öttinger (1995). A recent study illustrating another situation in which polymer molecules stretch to a contour length that is comparable to the characteristic dimension of the flow is the investigation of the dynamics of dilute solutions of DNA flowing in a scaled down roll-knife coating flow by Duggal *et al.* (2008). As mentioned earlier, kinetic theory models, such as the Hookean dumbbell model, are typically built on the assumption of homogenous fields, with negligible variation on the length scale of individual molecules. The findings by Bajaj *et al.* (2008) and Duggal *et al.* (2008) highlights the need to derive more refined models that are valid in non-homogeneous fields.

Insight into the nature of the maximum in the polymeric stress on the centreline in the cylinder wake can be obtained by examining the equation for the *xx*-component of the conformation tensor. It is straightforward to show that along the symmetry line equation (11) can be simplified at steady state to an ordinary differential equation for $M_{xx}$,

$$\frac{dM_{xx}}{dx} = -\frac{(1-2\lambda\kappa_{xx}(x))}{\lambda v_x(x)}M_{xx} + \frac{1}{\lambda v_x(x)} \tag{19}$$

where, $M_{xx}$ is the *xx*-component of the non-dimensional conformation tensor **M** defined by,

$$\mathbf{M} = \frac{1}{(\langle Q^2\rangle_{eq}/3)}\tilde{\mathbf{M}} \tag{20}$$

Since $dM_{xx}/dx = 0$ at the maximum in the wake, a simple relationship for the value of $M_{xx}$ at the maximum can be derived, which is denoted here by $x^*$,

$$M_{xx}|_{x=x^*} = \frac{1}{1-2\lambda\,\kappa_{xx}|_{x=x^*}} \tag{21}$$

This equation clearly implies that $M_{xx}$ becomes unbounded if $\lambda\kappa_{xx}$ approaches 0.5 at $x = x^*$. Using an FEM technique, Bajaj *et al.* (2008) examined the value of $\lambda\kappa_{xx}$ at the location of the maximum for both ultra-dilute and dilute polymer solutions.

For ultra-dilute solutions, their computations reveal that $\lambda\kappa_{xx}|_{x=x^*}$ approaches 0.5 as a power-law in *Wi*. As a result, $M_{xx} \to \infty$ only as $Wi \to \infty$, entirely in agreement with the earlier work by Wapperom and Renardy (2005). On the other hand, for dilute solutions, it was observed that $\lambda\kappa_{xx}|_{x=x^*} \to 0.5$ linearly in $Wi^{-1}$, independent of the choice of viscosity ratio $\beta$, as displayed in Fig. 9(a). This implies

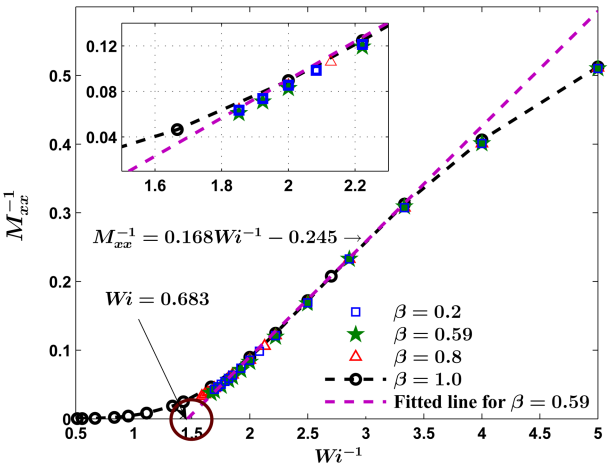


**Fig. 10.** Variation of the inverse polymer stretch $M_{xx}^{-1}$ for the Oldroyd-B model, at the location of the stress maxima in the cylinder wake, with inverse Weissenberg number $Wi^{-1}$, for ultradilute and dilute solutions. Reprinted figure with permission from M. M. Bajaj, M. Pasquali and J. R. Prakash, Journal of Rheology 52, 197-223, 2008. (http://dx.doi.org/10.1122/1.2807444).

that $M_{xx} \to \infty$ at a finite value of $Wi \approx 0.7$. This is clearly evident in Fig. 9(b), where the dependence of $M_{xx}$ on $\lambda\kappa_{xx}|_{x=x^*}$ is displayed for an Oldroyd-B fluid by the continuous blue line for $\beta = 0.59$. For dilute FENE-P liquids, on the other hand, Fig. 9(b) reveals that $M_{xx}$ increases relatively rapidly as $\lambda\kappa_{xx}|_{x=x^*}$ approaches 0.5, but levels off and remains bounded for higher values of $\lambda\kappa_{xx}|_{x=x^*}$. The shape of the curves are strongly suggestive of the occurrence of a coil-stretch transition in the cylinder wake.

With a view to examining whether $M_{xx}^{-1}$ approaches zero at a finite value of *Wi*, Bajaj *et al.* (2008) plotted the inverse of $M_{xx}$ versus the inverse of *Wi*, as displayed here in Fig. 10. The black dashed line for an ultra-dilute solution suggests that, as remarked above, $M_{xx}^{-1}$ goes to zero only as $Wi \to \infty$. On the other hand, for dilute solutions, the coupling of the flow and the polymer stress appears to lead to an upper bound for the existence of solutions. The data in Fig. 10 suggests that the maximum value is $Wi = 0.683$. Thus, for the first time, Bajaj *et al.* (2008) have presented evidence for an upper bound in *Wi* for the existence of solutions for the steady flow of an Oldroyd-B fluid around a cylinder confined between parallel plates. Interestingly, there are currently no mesh-converged results beyond $Wi = 0.7$ for steady flow around a confined cylinder.

It is worth noting, however, that the results of Bajaj *et al.* (2008) are limited to steady symmetric two-dimensional flow around a confined cylinder. Even though the stresses become singular in this particular scenario, a different type of solution to the Oldroyd-B model might arise in a dynamical situation, which is probably asymmetric and time-dependent.

Chilcott and Rallison (1988) suggested insightfully sev-

eral years ago that the flow modification near the rear stagnation point caused by the coupling of the spatial gradients of polymer structure with the fluid velocity field could be the source of the physical mechanism leading to the breakdown of the numerical solution. They argued that the increased velocity gradients near the rear stagnation point causes $M_{xx}$ to grow, which in turns feeds back to cause a greater increase in the velocity. While this cannot occur indefinitely for a FENE-P fluid, there is no mechanism to stop $M_{xx}$ from growing indefinitely for an Oldroyd-B fluid, leading to the ultimate breakdown of the solution.

While it is certainly true that FENE-P fluid simulations do not breakdown at the same small values of *Wi* as those observed for the Oldroyd-B fluid, they nevertheless do inevitably breakdown as *Wi* increases beyond some threshold value. This is because while the stress itself may not be singular, singularities might exist in stress *gradients*. In their recent paper, Becherer *et al.* (2009) suggest that for all constitutive equations which include stress advection and stress relaxation, but do not incorporate stress diffusion, localization of large stresses and stress gradients, and the existence of singular behaviour might be the typical feature of solutions near stagnation points. Clearly, therefore, the incorporation of finite extensibility alone does not lead to a resolution of all the difficulties associated with computing the flow of viscoelastic fluids.

Before finally discussing possible future directions for computing viscoelastic flows, additional physical phenomenon suggested by recent advances in the pursuit of the microscopic cycle which must be incorporated into the theoretical description of polymer solutions in order to obtain accurate predictions, are first discussed in the next section.

## 5. The Microscopic Cycle Revisited

We return to the microscopic cycle and continue our discussion of attempts to attain convergence between experiment and predictions in homogeneous flows. Many years of endeavour in this direction have made it clear that in order to obtain accurate predictions, two important pieces of physics have to be incorporated into microscopic models, namely hydrodynamic interactions (HI) and excluded volume (EV) effects (Bird and Öttinger, 1992; De Gennes, 1979; Doi and Edwards, 1986; Larson, 2004; Prakash, 1999; Shaqfeh, 2005).

As is well known, excluded volume interactions account for the fact that two parts of a polymer chain cannot occupy the same place at the same time. It is crucially important to include this phenomenon in the description of all solutions that are not at their $\theta$-temperature. For instance, the simple scaling relation between the radius of gyration and molecular weight of a polymer, $R_g \sim M^{0.6}$, observed for large molecular weight polymers in good solvents, cannot be predicted without the incorporation of EV effects. The theoretical treatment of EV effects in equilibrium solutions is very advanced, and remarkably accurate predictions of experimental observations have been obtained (De Gennes, 1979; Des Cloizeaux and Jannink, 1990; Doi and Edwards, 1986; Schäfer, 1999). While the description of EV effects in far from equilibrium situations is still in its infancy, a number of efforts have been made to incorporate them into the theoretical description (Larson, 2004). In particular, Prakash and co-workers have shown that a framework similar to that used to describe EV effects at equilibrium can also be used to describe their influence far from equilibrium, and parameter free predictions of a number of experimental observations can be obtained with such an approach (Prakash, 2001, 2002; Prakash and Öttinger, 1999; Sunthar and Prakash, 2005, 2006). In this paper, attention is restricted to the role played by hydrodynamic interactions in determining the rheology of dilute polymer solutions, and readers are referred to the review paper by Larson (2004) and the papers by Prakash and co-workers for a more complete description of far-from-equilibrium EV effects.

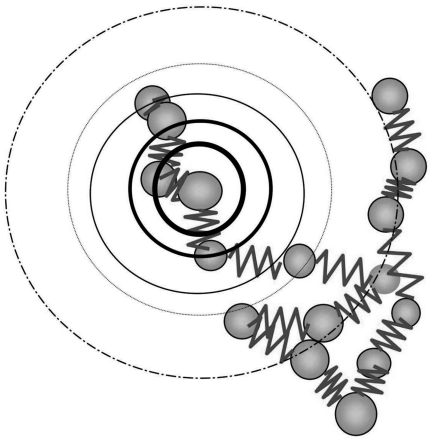

**Fig. 11.** Schematic representation of the effect of hydrodynamic interactions on a coarse-grained bead-spring chain model immersed in a solvent.

### 5.1. Hydrodynamic interactions

Hydrodynamic interactions describe the disturbance of the velocity field near all parts of a polymer chain due to the motion of any one part of the chain (as shown schematically in Fig. 11). This phenomenon couples together the motion of all the segments in a polymer molecule, and changes the drag force experienced by them due to their motion relative to the solvent. It turns out to be crucial to include HI to obtain an accurate description of any property whose definition depends on time, i.e., any dynamic property.

An example of a dynamic property which can be predicted accurately by including HI is the diffusivity *D*, which is proportional to the mean squared displacement of

a polymer molecule with time. If HI is neglected, it can be shown that the total frictional resistance to motion of the molecule is the sum of the frictional resistance from all the polymer segments (Bird *et al*., 1987b). As a result, the total frictional drag on the polymer scales linearly with molecular weight *M*. Since diffusivity varies inversely with drag, *D* scales as $M^{-1}$. On the other hand, if HI is included, it can be shown that the drag on the polymer scales as the size of the polymer molecule (Bird *et al.*, 1987b). In a $\theta$-solution at equilibrium, the size of a polymer molecule in the coiled state scales as the square root of molecular weight, and as a result, $D \sim M^{-1/2}$. This is exactly in agreement with observations.

Very roughly speaking, the inclusion of HI appears to ensure that the drag on a polymer molecule is calculated accurately. While the importance of estimating drag accurately was demonstrated quite early in the development of kinetic theory by Zimm (1956) for the prediction of an equilibrium property such as the diffusivity, and for predicting linear viscoelastic properties such as small amplitude oscillatory shear properties, it has recently become clear that accurately accounting for the conformational dependence of drag is extremely important even for properties far from equilibrium. Perhaps the most compelling demonstration of this has come out of attempts to predict the extraordinary manifestation of *hysteresis* in the behaviour of polymer solutions. In the subsection below, the phenomenon of coil-stretch hysteresis is discussed in some detail since it seems inevitable that an adequate recognition of its importance will eventually have paradigm changing implications for the modelling of polymer solution rheology. Before we do so, however, we summarize the equations used in polymer kinetic theory to describe HI within the context of bead-spring chain models.

Under homogeneous flow conditions, the configurational state of a bead-spring chain, with $N_s$ springs, is completely specified by the set of connector vectors $\{\boldsymbol{Q}_i | i = 1, \ldots, N_s\}$ (Bird *et al*., 1987b). The Fokker-Planck equation governing the evolution of the configurational probability distribution $\psi(\boldsymbol{Q}_1, \ldots, \boldsymbol{Q}_{Ns}, t)$ in the presence of hydrodynamic interactions is (Prakash, 1999),

$$\frac{\partial \psi}{\partial t} = -\sum_{i=1}^{N_s} \frac{\partial}{\partial \boldsymbol{Q}_i} \cdot \left\{ \boldsymbol{\kappa} \cdot \boldsymbol{Q}_i - \frac{1}{\zeta} \sum_{j=1}^{N_s} \tilde{\boldsymbol{A}}_{ij} \cdot \mathbf{F}_{c,j} \right\} \psi + \frac{k_B T}{\zeta} \sum_{i,j=1}^{N_s} \frac{\partial}{\partial \boldsymbol{Q}_i} \cdot \tilde{\boldsymbol{A}}_{ij} \cdot \frac{\partial \psi}{\partial \boldsymbol{Q}_j} \tag{22}$$

where, the dimensionless diffusion tensors $\tilde{\boldsymbol{A}}_{ij}$ are given by,

$$\tilde{\boldsymbol{A}}_{ij} = A_{ij}\boldsymbol{\delta} + \zeta(\boldsymbol{\Omega}_{ij} + \boldsymbol{\Omega}_{i+1,j+1} - \boldsymbol{\Omega}_{i,j+1} - \boldsymbol{\Omega}_{i+1,j}) \tag{23}$$

Here, $A_{ij} = \delta_{ij} + \delta_{i+1,j+1} - \delta_{i,j+1} - \delta_{i+1,j} = 2\delta_{ij} - \delta_{|i-j|,1}$ is an element of the $N_s \times N_s$ Rouse matrix, and $\Omega_{\nu\mu}$, $\nu$, $\mu = 1, \ldots, N$, are HI tensors, which are typically related to the inter-bead displacement $\boldsymbol{r}_{\mu\nu}$ between beads $\mu$ and $\nu$, by expressions of the form,

$$\boldsymbol{\Omega}_{\nu\mu} = \frac{1}{8\pi\eta_s r_{\mu\nu}} \boldsymbol{C}(\boldsymbol{r}_{\mu\nu}) \tag{24}$$

Models which neglect the influence of HI -such as the original bead-spring model of Rouse (Rouse, 1953)- can be interpreted as ones in which the tensor $\boldsymbol{C}$ is set to zero. Early models incorporating HI (Kirkwood and Riseman, 1948; Zimm, 1956) used the Oseen-Burgers form of the HI tensor, in which

$$\boldsymbol{C}(\boldsymbol{r}_{\mu\nu}) = \boldsymbol{\delta} + \frac{\boldsymbol{r}_{\mu\nu}\boldsymbol{r}_{\mu\nu}}{r_{\mu\nu}^2}. \tag{25}$$

Although the Oseen-Burgers description of HI is inaccurate when the pair-wise separation between beads is comparable to the size of the beads, the hydrodynamic behaviour of long polymer chains is dominated by the interactions between non-adjacent beads, and the short range inaccuracy of the Oseen-Burgers description has been shown to be relatively unimportant in the prediction of properties that depend on the polymer chain as a whole (Öttinger, 1987; Zimm, 1980). Further, its simple form is particularly useful for the development of closure approximations. In numerical simulations, however, the Oseen-Burgers expression becomes problematic when $r_{\nu\mu} \le a$, since the $3N \times 3N$ diffusion block-matrix comprising the $\tilde{\boldsymbol{A}}_{ij}$ tensors as its constituent blocks, can become non-positive definite (Rotne and Prager, 1969) when beads overlap. Typically, in Brownian dynamics simulations, the Rotne-Prager-Yamakawa (RPY) modification (Prabhakar *et al.*, 2004; Rotne and Prager, 1969; Yamakawa, 1971), which ensures that the diffusion block-matrix always remains positive-definite, is used in place of the Oseen-Burgers tensor.

Kramers' expression for the polymer contribution to the stress tensor $\boldsymbol{\tau}_p$ for bead-spring chains is given by (Bird *et al*., 1987b),

$$\boldsymbol{\tau}_p = -n_p \sum_{i=1}^{N_s} \langle \boldsymbol{Q}_i \mathbf{F}_{c,i} \rangle + n_p k_B T N_s \boldsymbol{\delta} \tag{26}$$

Consequently, the key to predicting rheological properties in the presence of HI is the evaluation of the configuration average $\langle \boldsymbol{Q}_i \mathbf{F}_{c,i} \rangle$, with the distribution function $\psi(\boldsymbol{Q}_1, \ldots, \boldsymbol{Q}_{Ns}, t)$ that satisfies the diffusion equation (22). As discussed in the case of the dumbbell model with a nonlinear spring earlier, two options are available in order to do this. The first is to write a stochastic differential equation which is equivalent to Eq. (22), and carry out BD simulations, and the other is to introduce closure approximations. The latter option is discussed in greater detail in subsection 5.4. We refer readers to Prabhakar and Prakash (2004) for a description of the stochastic differential equation that is

equivalent to Eq. (22), and for details of the BD algorithm that can be used to solve it.

The discussion of coil-stretch hysteresis is taken up in subsection 5.2 below. In the remaining subsections of section 5 we continue our discussion of the treatment of HI in the microscopic cycle, and how it can be incorporated into theoretical descriptions in the macroscopic cycle through the development of closure approximations.

### 5.2. Coil-stretch hysteresis

In a seminal paper more than three decades ago, De Gennes (1974) proposed arguments to suggest that under certain circumstances, the time history of deformation experienced by the solution might have a crucial bearing on the steady-state value of stress attained for a given deformation rate. The extraordinary implications of De Gennes contention for the modelling of polymer solutions was recognized at about the same time by Hinch and Tanner (Hinch, 1974; Tanner, 1975). Serious early doubts, however, about the theoretical validity of De Gennes arguments (Fan *et al.*, 1978; Wiest *et al.*, 1989), and the absence until recently of any supporting experimental evidence, has implied that the need for a fundamental change in the modelling of polymer solution rheology has not been widely recognized so far.

Recently, in ground breaking experiments, Shaqfeh and coworkers have shown that ultradilute solutions of DNA molecules subjected to planar elongational flow at identical rates of deformation, can have individual DNA molecules that are in two widely disparate conformational states – either coiled or highly stretched – depending on the time history of the solution's deformation (Schroeder *et al.*, 2003, 2004). Since the stress in a polymer solution has its origin predominantly in the entropic resistance of individual polymer molecules to deformation from their equilibrium coiled state, the Stanford group's results clearly validate De Gennes hypothesis (albeit indirectly) of different deformation histories leading to disparate states of stress. In addition, theoretical work by these authors and others (Darinskii and Saphiannikova, 1994; Hsieh *et al.*, 2005; Schroeder *et al.*, 2003, 2004) has also helped place the original arguments of De Gennes, Hinch and Tanner on a more rigorous footing.

The design of the flow cell used in the Stanford experiments, while being ideal for the observation of single molecules for extended periods of time, does not currently enable the simultaneous measurement of fluid stresses. In a recent paper, however, Sridhar *et al*. (2007) have reported for a synthetic polymer solution undergoing uni-axial elongational flow, the measurement of bulk stresses with appreciably different magnitudes at identical values of strain rate, depending on the time history of the solution's deformation. This demonstration has been achieved by extending the operation of the filament stretching rheometer from its usual constant strain rate mode, in two significant ways: (i) to a 'quench' mode of operation, where the strain rate is made to undergo a step change downwards from an initially high value, and (ii) to a constant stress mode of operation, where a uniform elongational flow field is generated in which a desired value of stress is achieved and maintained constant, while measurements of the resultant strain rate are made. Computer simulations have also been carried out by Sridhar *et al.* (2007) to mirror the experiments and are shown to support and enable the interpretation of the experimental observations, and indicate as conjectured originally by De Gennes, that the origin of the deformation history dependence of stress lies in the conformation dependence of hydrodynamic forces.

De Gennes original conclusions can be summarized quite simply with the help of the schematic in Fig. 12, where $\sigma$ is the steady state value of the stress in a dilute solution subjected to an elongational flow with strain rate $\dot{\varepsilon}$. At small values of $\dot{\varepsilon}$, polymer molecules are predominantly in a coiled state. However, with increasing $\dot{\varepsilon}$ a critical value of strain rate $\dot{\varepsilon}_{max}$ is reached at which the molecules undergo a sharp transition from a coiled to a stretched state, with a concomitant steep increase in the value of the steady-state stress. The rapidity of the transition increases greatly with increasing polymer molecular weight *M*. De Gennes' insight was to recognize that when the strain rate is incrementally decreased, on the other hand, from an initial value at which polymer molecules are in a stretched state, the critical strain rate $\dot{\varepsilon}_{min}$ at which the molecules return to a coiled state is not the same as $\dot{\varepsilon}_{max}$ but is noticeably smaller, with a difference that grows as the square root of molecular weight. As a result, for strain rates that lie between these two critical values, the solution's stress could correspond either to the coiled state value, or to the stretched state value, depending on the time history of deformation. Indeed, a third value of stress was also shown

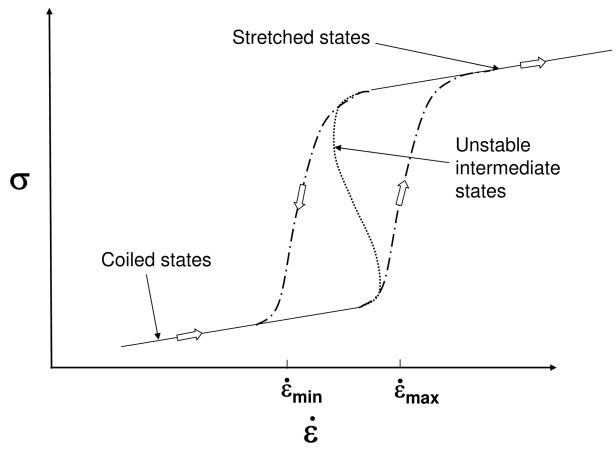


**Fig. 12.** Sketch of steady-state stress versus strain rate proposed by de Gennes, demonstrating the existence of hysteretic behaviour.

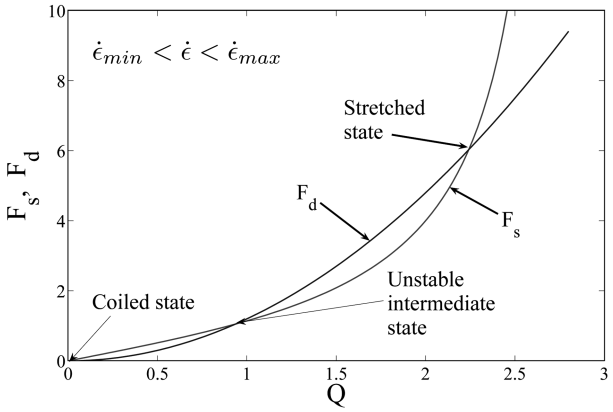


**Fig. 13.** Origin of coil-stretch hysteresis in the absence of Brownian forces. Nonlinear dependence of the spring and drag forces on polymer extension $Q$, at a particular value of strain rate within the hysteresis window, $\varepsilon_{\min} < \varepsilon < \varepsilon_{\max}$. Points of intersection indicate the three possible solutions to the force balance.

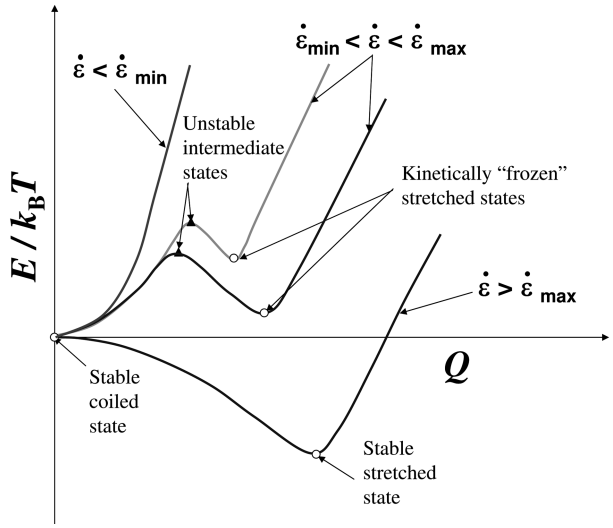


**Fig. 14.** Energy landscapes for strain rates in the neighbourhood of the hysteresis window, $\varepsilon_{\min} < \varepsilon < \varepsilon_{\max}$, indicating stable, kinetically frozen and unstable states.

to be possible in principle, that lies between these two states, but which is unstable. This hysteretic behaviour was attributed by De Gennes to arise due to the large change in the hydrodynamic drag force experienced by a polymer as it is unraveled from a coiled state to a stretched state. In the coiled state, the drag on a polymer is approximately equal to that on a sphere whose radius is equal to the radius of gyration of the polymer, $R_g$. In the stretched state, however, the drag is approximately equal to that on a slender cylinder, whose length is equal to the fully stretched length of the polymer chain, $L$.

A simple understanding of the origin of coil-stretch hysteresis for a single molecule subjected to an elongational flow, in the absence of Brownian forces, can be obtained by representing a polymer molecule by a dumbbell (Tanner, 1975). As indicated in Fig. 3, the hydrodynamic drag force on the polymer (modelled by the frictional force on the beads), is balanced by the resistance of the polymer molecule to deformation (modelled by the spring force between the beads). Equilibrium separation between the beads is attained when the drag force on the beads exactly balances the spring force between them. Since both the drag force and the spring force vary non-linearly with bead separation, it turns out that for strain rates between the critical values $\varepsilon_{\min}$ and $\varepsilon_{\max}$, three distinct solutions to the force balance exist. This is illustrated schematically in Fig. 13 as the points of intersection between the curves representing the spring and drag force, respectively (including the one at the origin, which corresponds to a coiled state). For strain rates in this hysteresis window, both the coiled and stretched state solutions are stable, with the intermediate solution being unstable. As a result, for an initially stretched molecule, as the strain rate is decreased below $\varepsilon_{\max}$ from above, the force balance is satisfied with the polymer remaining in a stretched state, with a transition to a coiled state only occurring when the strain rate falls below $\varepsilon_{\min}$ (see Fig. 12). Such is not the case for strain rates below $\varepsilon_{\min}$ or above $\varepsilon_{\max}$, where only a single solution for the equilibrium bead separation is stable, corresponding to either the coiled or the stretched state, respectively. For an initially coiled molecule, as the strain rate is increased incrementally above $\varepsilon_{\min}$ from below, the force balance is satisfied with the polymer remaining in a coiled state for $\varepsilon_{\min} < \varepsilon < \varepsilon_{\max}$, with a rapid transition to the stable stretched state solution, when $\varepsilon > \varepsilon_{\max}$.

A serious and valid argument against the possible existence of multiple steady-states proposed by De Gennes was made by Fan *et al*. (1978), who pointed out that since the Fokker-Planck equation governing the distribution of configurations of a chain is linear in the distribution function, only a unique distribution function is admissible as a solution at any particular extension rate, leading to a unique steady-state value for any macroscopic property. According to Fan *et al.* (1978), it was the use by De Gennes of approximations that made the governing equations nonlinear in the distribution function, that was the source of the incorrect postulation of the existence of multiple steady-states.

In his original paper, De Gennes had also proposed an alternative framework within which it is possible for hysteretic behaviour to be observed, which does not suffer from the shortcomings pointed out by Fan *et al.* (1978). Fig. 14 is a schematic representation of this alternative picture within which a polymer molecule's behaviour is examined in terms of its conformational free energy. For strain rates $\varepsilon > \varepsilon_{\max}$, the stretched state is the lowest energy state, while for strain rates $\varepsilon < \varepsilon_{\min}$, the coiled state is the lowest energy state. However, for strain rates between $\varepsilon_{\min}$

and $\varepsilon_{max}$, even though the coiled state (at the origin) is a lower energy state, an initially stretched molecule is kinetically "frozen" in a stretched state because of a large energy barrier that separates the stretched and coiled states. As a result, when the strain rate is decreased from a value above $\varepsilon_{max}$ to a value within the hysteresis window, and provided that the energy barrier between the two stable states is sufficiently large, the measured stress in a polymer solution undergoing extensional flow would correspond to an ensemble of molecules that are not distributed according to the "ergodic" steady-state distribution at that strain rate, but rather are distributed over an ensemble of "frozen" configurations. Since this "frozen" ensemble would be entirely different when the solution is extended at the same strain rate but starting with initially coiled molecules, stress hysteresis would be observed.

It is worth noting that within this picture of the dynamics of coil-stretch transition, there are two scenarios in which hysteresis will not be observed. The first is one in which the energy barrier separating the coiled and stretched states is not large relative to thermal energy. In this case, molecules would rapidly transit between the two states, leading to an ergodic sampling of all possible conformational states, and a unique value for any property obtained as a conformational average. The second is one in which the experimental observation is made over an infinitely long period of time. In this case, even though polymer molecules are "frozen" in certain conformational states, with a significant slowing down in their dynamics, ultimately the ensemble of molecules will be distributed over all possible states, with a unique conformational average. These arguments suggest therefore that the size of the hysteresis window is a function both of the energy barrier between states, and the duration of experimental observation.

The experimental observations by Shaqfeh and coworkers (Schroeder *et al*., 2003, 2004) of the simultaneous existence of both coiled and stretched states of E-coli DNA, for as many as $\varepsilon = 15$ Hencky strain units (where, $\varepsilon \equiv \dot{\varepsilon} t$), and the clear delineation of the hysteresis window at $\varepsilon = 15$, lends strong support to De Gennes visualization of coil-stretch hysteresis in terms of polymer molecules hopping between states in the conformational energy landscape.

In addition, results of Brownian dynamics simulations of bead-spring chains, in which hydrodynamic interactions are included along with finitely extensible springs, carried out by Shaqfeh and coworkers (Beck and Shaqfeh, 2006; Schroeder *et al*., 2003, 2004) and Hsieh and Larson (Hsieh *et al*., 2005), are entirely consistent with the interpretation of experimental observations within this framework. If the critical Weissenberg number for coil-stretch transition $Wi_c$ is defined as $Wi_c \equiv \lambda_1 \varepsilon_{max}$, where $\lambda_1$ is the longest relaxation time of the polymer, then simulations and experiments indicate that $Wi_c \approx 0.5$ (Hsieh *et al*., 2005; Schroeder *et al*., 2003, 2004). For simulations very close to $Wi_c$, Shaqfeh and coworkers observed the simultaneous existence of

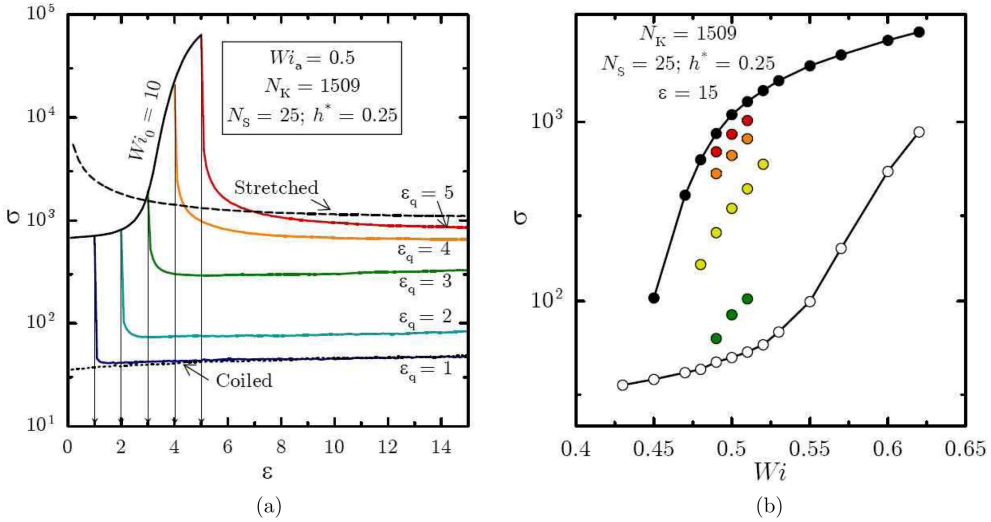


**Fig. 15.** Glassy dynamics at the critical Weissenberg number. (a) Stress evolution. The dotted and dashed lines indicate the evolution of the total stress as a function of Hencky strain during the imposition of a constant non-dimensional strain rate $Wi = 0.5$, starting from equilibrium and 90% fully-stretched initial configurations, respectively. In the quench simulations, an initial strain rate corresponding to $Wi_0 = 10$ is imposed until a desired value of the strain (indicated by the arrows) is reached, and then Wi is instantaneously decreased to 0.5. (b) Hysteresis in the total stress at a Hencky strain of $\varepsilon = 15$. Filled black circles are obtained from simulations with the extension rate maintained constant, with the chains initially stretched to 90% of their fully stretched length. Empty circles are from simulations with a constant extension rate, with the initial configuration of the ensemble of chains chosen from the equilibrium configurational distribution. Symbols within the hysteresis window correspond to quasi-steady-state values of stress attained with simulations that quench to various values of the Weissenberg number, from $Wi_0 = 10$.

coiled and stretched states for over 50 Hencky strain units (Schroeder *et al.*, 2003, 2004). On the other hand, for Weissenberg numbers slightly larger (smaller) than $Wi_c$, initially coiled (stretched) molecules gradually unravel (collapse) to a stretched (coiled) state. By considering a single molecule's trajectory over nearly 1000 strain units, Hsieh *et al.* (2005) were able to observe the dependence of the hopping frequency between coiled and stretched states on the Weissenberg number, and found the behaviour to be in qualitative agreement with the simulation results of Schroeder *et al.* (2003, 2004). More recently, Beck and Shaqfeh (2006) have shown that the hysteretic behaviour of a polymer molecule tethered at a surface stagnation point can be systematically understood in terms of state hopping within a double-welled potential, and have used this model to derive an analytical expression for the hopping rate based on Kramers rate theory. Interestingly, in this case, the non-linearity in the drag experienced by the unraveling polymer molecule is caused by the presence of a non-uniform flow on the length-scale of the polymer molecule.

It is appropriate to note here that both Beck and Shaqfeh (2006) and Hsieh *et al.* (2005) show through simulations that the width of the hysteresis window increases with increasing chain length. Additionally, the former authors have also shown that the window width decreases with increasing duration of observation, and that the energy barrier between the two stable states increases exponentially with chain length.

The experiments and computational results of Shaqfeh and coworkers present a compelling picture of the dynamics of coil-stretch transition. However, they are all restricted to single molecule studies. The recent work by Sridhar *et al.* (2007) addresses a number of important issues that can be examined more fruitfully from the perspective of bulk measurements. For instance, it is not clear from single molecule experiments whether the existence of disparate conformational states is sufficient to cause observable hysteretic behaviour in measurements of the bulk stress, which is a property that is evaluated over an ensemble of molecules that are likely to be distributed over a range of conformations. Secondly, since hopping between coiled and stretched states occurs across large energy barriers within the hysteresis window, the time evolution of all macroscopic properties can be expected to be considerably slowed down in this regime. Finally, if the rate of deformation of a polymer solution is suddenly quenched into the hysteretic regime, then the population of molecules immediately after the quench can be expected to be rapidly partitioned into the two wells corresponding to the coiled and stretched states, followed by a slow evolution depending on the strain rate after quenching. This would lead to a strong dependence of the measured stress on the distribution of chain configurations at the instant prior to quenching, and consequently, even though the strain rates are identical after the quench, a wide variety of stresses can be expected depending on the deformation history. Sridhar *et al.* (2007) have carried out experiments and computer simulations to examine these issues, and their results are summarized below.

Since the results of BD simulations assist considerably in the interpretation of experimental observations, these are discussed first. A bead-spring chain model with finitely extensible springs and hydrodynamic interactions has been used by Sridhar *et al.* (2007), and details of the BD algorithm used by them can be found in Prabhakar and Prakash (2004). Basically, three different protocols have been adopted by Sridhar *et al.* (2007) for the simulation of uniaxial elongational flow, as described in the caption to Fig. 15.

Fig. 15(a) displays the total stress in the polymer solution as a function of strain in uniaxial extensional flow. The dotted line, corresponding to the transient response of an ensemble of initially coiled molecules, can be seen to gradually increase and level off to a value that remains constant for a large number of strain units, representing a quasi-steady-state. The dashed line in Fig. 15(a) represents the stress evolution of an ensemble of initially stretched chains. After a rapid decrease at small strains because of a reduction in the stretch of the molecules from their initial nearly fully stretched values, the stress remains constant for a large number of strain units at a quasi-steady-state value significantly higher than that corresponding to the coiled state stress. As a result, the simulations clearly indicate the existence of hysteresis in the bulk stress analogous to the coil-stretch hysteresis observed earlier in simulations and experiments.

The quench simulations clearly show the existence of glassy dynamics within the hysteresis window. All the stress profiles have a common pattern of a rapid drop in stress subsequent to the quench, followed by a nearly constant value for an extended period of time. As may be expected, with increasing strain chains become increasingly stretched, and the distribution of conformations changes from being predominantly coiled to predominantly stretched. A quench from each of these strains therefore corresponds to a different initial population of chain conformations. For instance, a quench at $\varepsilon = 1$, where the chains are still mostly coiled, leads to a quasi-steady-state stress value close to that obtained from a constant strain rate simulation carried out with initially coiled molecules. In contrast, the initially high Weissenberg number, $Wi_0 = 10$, leads to a population of predominantly stretched chains by $\varepsilon = 5$, such that a quench at this value of strain leads to a quasi-steady-state stress which is close to that obtained from a constant strain rate simulation carried out with initially nearly fully stretched molecules. Quenches carried out at intermediate strains lead to quasi-steady-state stresses that lie between these two extremes. The final value of stress is clearly related to the ratio in which the chains are partitioned into

the two energy wells. In short, at a Weissenberg number of 0.5, depending on the time history of deformation, the quasi-steady-state stress value can lie anywhere between the two limiting values attained with constant strain rate simulations that start with initially coiled or initially stretched molecules, respectively.

Fig. 15(b) graphically demonstrates both the existence of hysteresis in the bulk stress, and the multiple values of stress that can be attained at any particular Weissenberg number within the hysteresis window. While the filled black and empty circles were obtained with constant strain rate simulations that start with initially stretched and initially coiled molecules, respectively, symbols lying between them were obtained with simulations that quench from $Wi_0 = 10$ to various values of the Weissenberg number within the hysteresis window.

It is important to bear in mind that Fig. 15(b) is a snapshot of the dynamics of coilstretch transition at $\varepsilon = 15$, and that a similar set of data displayed at a larger value of $\varepsilon$ would be different. This can be understood by considering Fig. 15(a). If the various lines representing quasi-steady-state values of stress were extended indefinitely to the right, then they would all converge to a single line, representing the unique steady state value of stress at $Wi = 0.5$. This is because molecules that are trapped in the two wells at $\varepsilon = 15$ will slowly hop and redistribute themselves ergodically, giving rise to a unique value of stress. This would translate in Fig. 15(b) to a shrinking of the hysteresis window with increasing observation strain $\varepsilon$ until a unique sigmoidal stress versus Weissenberg number curve is obtained. The central issue from a practical point of view of course is the rate at which this final 'true' steady state is obtained, which is clearly a function of the height of the energy barrier between the coiled and stretched states, and is reflected in the post-quench slope of the various stress versus strain lines in Fig. 15(a). Simulation results of the Stanford group clearly indicate that the energy barrier is a very strongly increasing function of the length of the molecule, and that the true steady state for typically encountered molecular weights may be unreachable in any time scale of experimental interest.

Fig. 16(a) is a composite plot of data for quasi-steady dimensionless stress $\sigma^* = \sigma/(n_p k_B T)$ against the Weissenberg number $Wi = \lambda_1 \dot{\varepsilon}$, reported by Sridhar *et al.* (2007) for a solution of polystyrene of molecular weight $1.12\times10^6$. The data in Fig. 16(a) were obtained using three different experimental protocols which mirror the simulation protocols, as described in the caption to Fig. 16.

The white circles form a lower bound for the quasi-steady stress measurements. This is consistent with the De Gennes' picture, as initially coiled molecules are likely to remain in the coiled-state energy basin and thus manifest lower values for the stress. At high strain rates [Fig. 16(a) inset], the data from the constant stress experiments (black

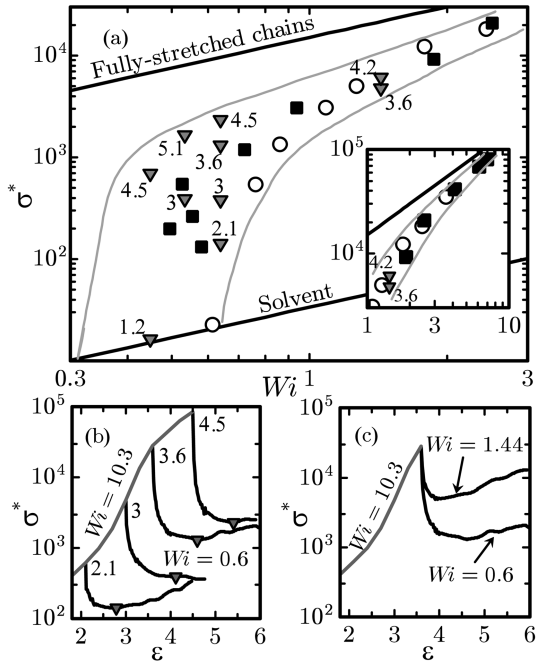


**Fig. 16.** (a) Quasi-steady state stress measurements demonstrate glassy dynamics associated with the coil-stretch transition. The grey lines in (a) outline the coil-stretch hysteresis window. The inset in (a) shows data at high strain rates. The data shown in (a) have been obtained with three different protocols: constant imposed strain-rate (white circles), constant imposed total stress (black squares) and strain-rate quench (grey triangles). The numbers alongside the grey triangles report the Hencky strains at quench. (b) Transient dimensionless stress in strain-rate quench experiments. (c) Slowing down of post-quench dynamics with decrease in quenched strain-rate. Reprinted figure with permission from T. Sridhar, D. A. Nguyen, R. Prabhakar and J. R. Prakash, Physical Review Letters, 98, 167801, 2007. (http://link.aps.org/doi/10.1103/PhysRevLett.98.167801). Copyright 2009 by the American Physical Society.

squares) are close to those obtained in the constant strain-rate experiments. In sharp contrast, however, at the lower strain rates, we see that the data from the two protocols do not collapse onto a single curve. This suggests that the polymer solutions at these strain rates have not reached true steady states within the experimental observation time, and that hysteresis is manifested in this regime of strain rates. The profile of the evolution of the stress in Fig. 16(b) in all the quench experiments, is very similar to that observed earlier with BD simulations (see Fig. 15(a)), with a rapid drop in stress after the quench, followed by a period of nearly constant stress which corresponds to a quasi-steady-state. The triangle symbols in Fig. 16(a) denote the post-quench plateau stress/strain-rate data obtained in these experiments. The numbers alongside the triangle symbols indicate the Hencky strains at quench. Fig. 16(a) displays

the experimental confirmation of the presence of multiple quasi-steady-states, and closely mirrors the results of simulations reported in Fig. 15(b).

Fig. 16(c) shows the evolution of stress in one particular quench experiment where the post-quench $Wi > Wi_c$. The stress is observed to rapidly decrease after the quench in line with expectation. However, after dropping to a minimum, it again begins to gradually increase giving rise to the appearance of an undershoot. Both the rapid drop in stress, and the slow increase can be understood by considering the configurations of a chain prior to quench in the context of the energy landscape in Fig. 14. Clearly, chains stretched beyond the effective stretched-state energy minimum prior to quenching appear to fall back into the stretched state energy well during the post-quench period, giving rise to the rapid drop in stress immediately after quench, observed in all the quench simulations and experiments. On the other hand, chains between the coiled and stretched-state energy wells are partitioned between the two depending on their configurations prior to quenching. These chains contribute to the slow evolution of stress in the post-quench period. For $Wi > Wi_c$, since the energy barrier for coil-to-stretch transitions is expected to be less than that for stretch-to-coil transitions, the stress will increase as the chains slowly hop from the coiled state into the stretched state, while the reverse behaviour can be expected for $Wi < Wi_c$.

Nearly all currently popular models in polymer rheology assume that the stress in a polymer solution is uniquely determined by the rate of deformation to which the solution is subjected. Yet, as clearly demonstrated by the experimental observations and computer simulations discussed above, under certain circumstances, the time history of conformational changes experienced by the molecules in a solution has a significant bearing on the value of stress attained for a given deformation rate. The demonstration recently by François *et al.* (2009) of the existence of stress and conformational hysteresis in the transcient flow around a cylinder of PEO polymer solutions suggests that stress hysteresis might be ubiquitous in complex flows. The accurate estimation of the relationship between stress and strain in a solution lies at the heart of being able to develop a realistic description of the flow of polymer solutions. Clearly, there is a need for a fundamental change in the modelling of polymer solution rheology. In particular, there is a need to recognize that constitutive equations that account for the conformational dependence of the drag experienced by individual molecules must be adopted in order to be able to predict more accurately the rich behaviour observed in the flow of polymer solutions. It turns out that it is indeed possible to develop constitutive equations at the macroscopic scale that account for hydrodynamic interactions, and thus the conformation dependence of drag. This will be discussed shortly in section 5.4 below. Before we do so, however, we first consider the rational choice of parameters in the bead-spring chain models that have been shown to be so successful in obtaining qualitative agreement with the experimental observations of hysteresis described above.

### 5.3. Successive fine graining

It is clear from the discussion so far that the incorporation of excluded volume effects is necessary in order to accurately predict properties in good-solvents, while the incorporation of hydrodynamic interactions, is required to predict dynamic properties. In addition, far from equilibrium, it has been found necessary to replace the Hookean springs of the beadspring chain model with finitely extensible springs in order to capture the shear thinning exhibited by the shear viscosity, and the boundedness of the elongational viscosity (Bird *et al*., 1987b). The incorporation of each of these phenomena, leads to the introduction of at least one new parameter into the theory. For instance, the pairwise strength of excluded volume interactions between any two beads in the bead-spring chain, is typically represented by the non-dimensional parameter $z^*$, which is proportional to $(1-T_\theta/T)$, where, $T$ is the solution temperature, and $T_\theta$ is the $\theta$-temperature of the polymer-solvent system. The strength of hydrodynamic interactions, on the other hand, is usually measured in terms of the magnitude of the parameter $h^*$, the non-dimensional bead radius. Finally, the inclusion of finitely extensible springs, introduces the parameter $b_M$, which, as we have seen, is a non-dimensional measure of the fully stretched length of a spring. Not surprisingly, for any particular choice of the number of beads $N$, a proper choice of the values of these parameters, turns out to have a crucial bearing on the accuracy of the predictions of any theory. Often, the correct values of the parameters to use in simulations is determined by essentially finding a best fit to experimental data, in some limiting regime of behavior (Hsieh *et al*., 2003; Jendrejack *et al*., 2002; Larson *et al*., 1999). While this procedure is a reasonable scheme for parameter estimation, it is not clear that the chosen set of values is unique, and that an alternative set of parameter values will not yield equally accurate predictions of either equilibrium or non-equilibrium properties. Furthermore, a simultaneous fit of all the parameters to experimental results does not recognize the fact that a few of the parameters have no influence on some of the experimental variables. For instance, the parameter $h^*$ has no influence on static equilibrium properties.

An alternative approach to the problem of parameter estimation has been developed by Prakash and coworkers by exploiting the universal behavior exhibited by dilute polymer solutions (Prabhakar *et al.*, 2004; Sunthar and Prakash, 2005). As is well known, the observed universal behavior has its origins in the self-similar nature of long chain flexible macromolecules in the coiled state. For equilibrium static and dynamic properties, Kröger *et al.* (2000) and

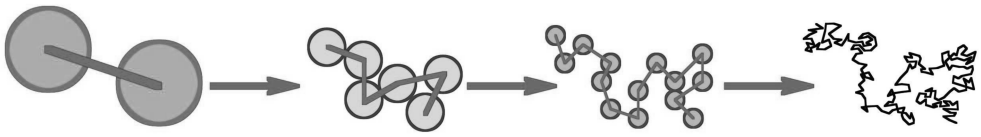

**Fig. 17.** Schematic representation of the SFG procedure.

Kumar and Prakash (2003) have previously established the methodology for obtaining exact predictions of universal properties from Brownian dynamics simulations. Both these procedures require the accumulation of data for increasing values of the number of beads $N$, and the subsequent extrapolatiion of the finite chain data to the limit $N \to \infty$. Basically, as more and more springs are included in the bead-spring chain, local details of the chain become immaterial, leading to parameter free predictions in the infinite chain length limit. Prakash and coworkers (Prabhakar *et al.*, 2004; Sunthar and Prakash, 2005) have adopted a modified version of this procedure for predicting behaviour in far from equilibrium situations since the finite contour length of the chain is a crucial determinant of solution properties in both shear and extensional flows at high deformation rates. In the case of finite chains, the simulation data for various increasing values of $N$ is extrapolated to the limit $N_s \to N_k$, rather than to the limit $N \to \infty$, since the maximum number of springs, $N_s$, that one can use is equal to the number of Kuhn steps $N_k$ in the underlying chain. Since increasing values of $N$ represent more fine-grained versions of the underlying chain, the procedure is called "*successive fine-graining* (SFG)." A schematic representation of the SFG procedure is shown in Fig. 17. Note that an important aspect of SFG is that certain key variables, such as the Weissenberg number *Wi* etc, are kept invariant in the fine-graining process (Prabhakar *et al.*, 2004; Sunthar and Prakash, 2005). By showing that predictions obtained with bead-spring chains and SFG agree very well with the BD results in shear and extensional flows obtained by Liu *et al.* (2004) using a bead-rod model, Pham *et al.* (2008) have recently convincingly established the validity of the SFG procedure.

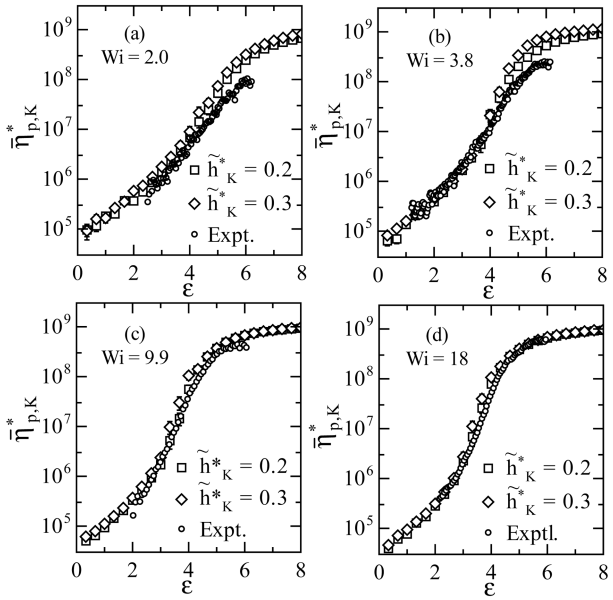


**Fig. 18.** Comparison of parameter-free predictions obtained with SFG of the growth of the dimensionless extensional viscosity with the experimental data of Gupta *et al.* (2000) (small circles). Simulations have been carried out for two different values of the hydrodynamic interaction parameter. Reprinted figure with permission from R. Prabhakar, J. R. Prakash and T. Sridhar, Journal of Rheology, 48, 1251-1278, 2004. (http://dx.doi.org/10.1122/1.1807841). Copyright 2009 by the Journal of Rheology.

Interestingly, experimental observations suggest that for a very large number of polymer-solvent systems, universal static and dynamic properties, independent of molecular weight and chemistry, are attained by relatively small values of molecular weight $M$. By comparing finite chain results with predictions in the universal long chain limit (through a careful examination of the role of finite size effects, and sensitivity to the choice of parameter values), Sunthar and Prakash (2005) have established using SFG that, even in the presence of flow, parameter free behaviour is obtained for finite chains with relatively small values of chain length $N_k$.

Fig. 18 compares predictions using SFG with the experiments of Gupta *et al.* (2000) on polystyrene solutions undergoing extensional flow. The excellent agreement between theory and experiments, obtained without any arbitrary choice of simulation parameters, suggests that at least with regard to treatment of finite extensibility and hydrodynamic interactions we are close to achieving convergence between theory and experiment in the microscopic cycle.

The question then is how does one translate this success to the macroscopic cycle. One of the ways is to use closed form constitutive equations.

### 5.4. Closure approximations

The need for a closure approximation upon the incorporation of finitely extensible springs and hydrodynamic interactions into the bead-spring chain model can best be seen from the following set of evolution equations for the second moments of the probability distribution $\psi$:

$$\frac{d}{dt}\langle \boldsymbol{Q}_i\boldsymbol{Q}_j\rangle = \boldsymbol{\kappa}\cdot\langle \boldsymbol{Q}_i\boldsymbol{Q}_j\rangle + \langle \boldsymbol{Q}_i\boldsymbol{Q}_j\rangle\cdot\boldsymbol{\kappa}^T + \frac{2k_BT}{\zeta}\langle \tilde{\boldsymbol{A}}_{ij}\rangle - \frac{1}{\zeta}\sum_{m=1}^{N_s}\langle \boldsymbol{Q}_i\mathbf{F}_{c,m}\cdot\tilde{\boldsymbol{A}}_{mj} + \tilde{\boldsymbol{A}}_{im}\cdot\mathbf{F}_{c,m}\boldsymbol{Q}_j\rangle \quad (27)$$

**Table 1.** Acronyms used for referring to various closure approximations in Fig. 19

| Treatment of HI | Acronym | Treatment of Finite Extensibility | Acronym |
|---|---|---|---|
| Free-draining | FD | Hookean springs | H |
| Equilibrium-averaging | EA | Peterlin | P |
| Consistent-averaging | CA | Peterlin/Gaussian | PG |
| Gaussian approximation | GA | | |

which can be derived from Eq. (22) by multiplying both sides by $\boldsymbol{Q}_i\boldsymbol{Q}_j$ and integrating over all configurations of the chain. Clearly, these equations are not closed for the second moments $\langle \boldsymbol{Q}_i\boldsymbol{Q}_j \rangle$ because of the appearance of complex moments on the right-hand-side, which involve both the nonlinearities introduced by the spring force law and HI.

Interestingly, nearly all the closure approximations that have been introduced in the literature so far can be derived from Eq. (27) by making the appropriate assumptions and simplifications. For instance, the first closure approximation for HI within the context of bead-spring chain models, the well known Zimm theory (Zimm, 1956), can be derived from Eq. (27) by using Hookean springs (so that $\mathbf{F}_{c,j} = H\boldsymbol{Q}_j$), and replacing the Oseen tensor $\boldsymbol{\Omega}_{\nu\mu}$ with its equilibrium average. The limitation of the accuracy of Zimm theory to linear viscoelastic property predictions has been the motivation for the development of more sophisticated treatments of HI. For instance, while the consistent averaging approximation (Öttinger, 1987) replaces the equilibrium averaged Oseen tensor in Zimm theory with a non-equilibrium average, the Gaussian approximation (Öttinger, 1989; Wedgewood, 1989) further accounts for fluctuations in HI. The Gaussian approximation, which is the most sophisticated approximation to date, has been shown to be highly accurate by comparing its predictions of viscometric functions with exact Brownian dynamics simulations (Zylka, 1991). We have previously discussed the Peterlin approximation for finitely extensible chains, which enables the derivation of closed form equations in the absence of HI. Wedgewood and Öttinger (1988) introduced a closure approximation for the situation when both finitely extensible springs and HI are present by combining the consistent averaging scheme for HI with a FENE-P approximation for the springs. More recently, Prabhakar and Prakash (2006) have introduced an approximation that extends the previously established Gaussian approximation by accounting for fluctuations in *both* HI and the spring forces. The accuracy of this model has been verified by comparison with BDS in a number of both transient and steady, shear and extensional flows.

Of all the various dilute polymer solution properties that can be accurately predicted by closure approximations for chains with HI, the ability of the more sophisticated approximations to predict multiple steady-state values for the extensional viscosity for a range of values of the non-dimensional extension rate $\varepsilon^*$ is perhaps one of the most compelling reasons for adopting them more widely in macroscopic simulations. Fig. 19 displays a comparison of the predictions of coil-stretch hysteresis by various closure approximations with the results of exact BD simulations. The meanings of the different acronyms used in the figure are given in Table 1. It is seen that with the notable exception of the EA-P model (Zimm + FENE-P), the predicted non-dimensional polymer contribution to the extensional viscosity ($\eta_p^*$) versus $\varepsilon^*$ curve exhibits coil-stretch hysteresis for all the other approximations for chains with HI. The predictions of the GA-P model are quite close to the BD simulation data.

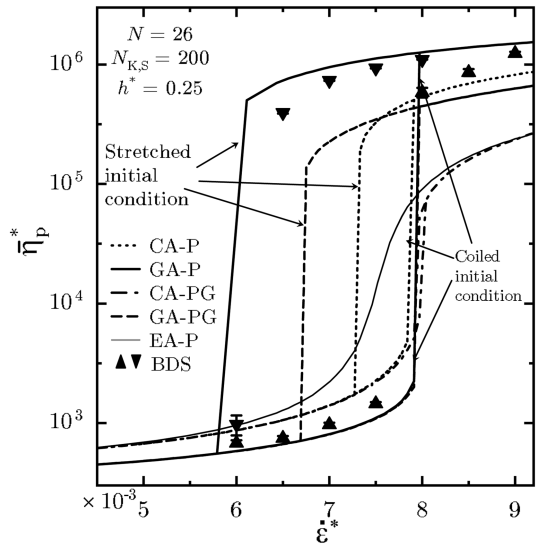


**Fig. 19.** Prediction of coil-stretch hysteresis in the steady-state extensional viscosity by closure approximations for finitely extensible bead-spring (FEBS) chains with HI. The upright and inverted triangle symbols represent BDS data obtained by successively stepping up, and stepping down, the extension rate, respectively. Meanings of the different acronyms are given in Table 1. Reprinted figure with permission from R. Prabhakar and J. R. Prakash, Journal of Rheology, 50, 561-593, 2006. (http://dx.doi.org/10.1122/1.2206715). Copyright 2009 by the Journal of Rheology.

The BDS results obtained by Schroeder *et al.* (2003), and those in Fig. 19 suggest that the exact distribution of the steady-state extensional stress in finitely extensible bead-spring (FEBS) chains with HI is bi-modal. The linearity of

the Fokker-Planck equation [Eq. (22)] in the configurational probability distribution function further guarantees that its exact solution is unique. The introduction of any mean-field approximation however leads to a modified Fokker-Planck equation that is nonlinear in the probability distribution function, since the coefficients in the modified Fokker-Planck equation are functionals of the distribution function. While the solution of this modified equation is a uni-modal Gaussian distribution, the nonlinearity in the distribution function means that the solution may no longer be unique. Thus, the exchange of the nonlinearities due to FENE and HI for a nonlinearity in the distribution function destroys the multi-modal nature of the original solution, but allows the modified Fokker-Planck equation to have multiple solutions. In spite of this fundamental difference between the exact and approximate probability distributions, the results presented in Fig. 19 above indicate that the multiple steady-states obtained with the approximations can closely follow the long-lived kinetically trapped states in the original model. Therefore, closure approximations for FEBS chains with HI can prove to be useful in a detailed exploration of hysteretic phenomena caused by ergodicity-breaking in dilute polymer solutions.

It is appropriate to note here that the Gaussian approximation has also been developed for the treatment of excluded volume interactions, and predictions have been compared with exact BD simulations. While the qualitative behaviour of a range of material functions is captured accurately, quantitative agreement is found only within a certain range of parameter values (Prakash, 2001, 2002; Prakash and Öttinger, 1999). It is also possible to treat the combined influence of HI and EV effects with a closure approximation, as demonstrated by Prabhakar and Prakash (2002b), who developed a Gaussian approximation for a dumbbell model. A comprehensive closure model for all the three nonlinear phenomenon of finite extensibility, excluded volume and hydrodynamic interactions has not been developed so far.

As an example of a complex fluid mechanical problem that can be addressed with the help of a sophisticated closure approximation, Prabhakar *et al.* (2006) have recently examined the elasto-capillary thinning and break-up of a thin filament of a dilute polymer solution, using a closure approximation which includes the effects of finite chain extensibility and configuration-dependent intramolecular hydrodynamic interaction. Their results clearly indicate that the configuration dependence of intramolecular hydrodynamic interactions plays an important role in determining the thinning dynamics. In a seminal study, Entov and Hinch (1997) had shown previously, using a simpler constitutive model that does not account for configuration-dependent hydrodynamic interactions, that during the period where the elastic polymer stresses are dominant, the filament radius decreases exponentially with time, and the Weissenberg number extracted from the rate of decrease of the filament radius reaches a plateau value of 2/3. In contrast, Prabhakar *et al.* (2006) observe that when the influence of configuration-dependent hydrodynamic interactions is accounted for in the constitutive model, the plateau value of Wi does not approach any clear limiting value, but is dependent on the key parameters characterizing the solution. Indeed, *Wi* appears to dip below the critical value for the coil-to-stretch transition in extensional flows, with a stabilization of the filament at sub-critical values of *Wi* due to coil-stretch hysteresis. Most interestingly, configuration-dependent hydrodynamic interactions are shown to cause the time-constant in the exponential-decay to depend on concentration. This dependence has been observed in recent experiments, and has been the source of some puzzlement (Clasen *et al*., 2006, 2004).

## 6. Micro-macro Simulations

So far we have discussed progress and problems in the development of complex fluid mechanics within the context of the microscopic and macroscopic cycles. In recent years an alternative approach to complex fluid mechanics has arisen that completely sets aside the paradigm described in Fig. 1. In this approach, which is called the micro-macro simulation approach, the microscopic scale of kinetic theory is coupled directly to the macroscopic scale of continuum mechanics, as illustrated in the schematic diagram displayed in Fig. 20. Typically, in most numerical algorithms that adopt this methodology, the conservation laws are solved by a standard finite element method for the velocity and pressure fields, with the polymer contribution to the stress, $\boldsymbol{\tau}_p$, taken to be a known body force term in the momentum balance. In turn, the value of $\boldsymbol{\tau}_p$ is calculated by carrying out an average over an ensemble of coarse-grained model molecules distributed over the flow domain, whose instantaneous configurations are computed by integrating stochastic differential equations subject to the flow field obtained by solving the conservation laws. The first implementation of this micro-macro simulation approach

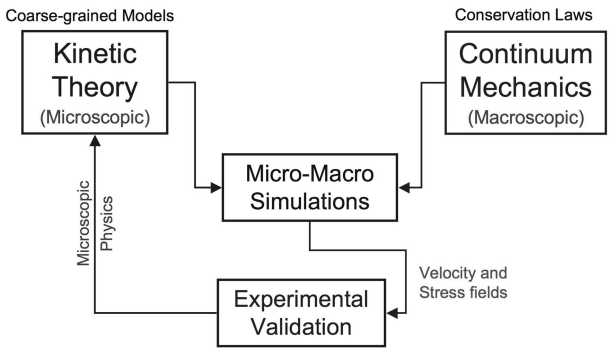


**Fig. 20.** Schematic representation of the micro-macro simulation methodology.

was by Laso and Ottinger (1993) with the so-called CONNFFESSIT method. A number of difficulties associated with this approach were resolved through the development of the Brownian configuration fields method by Hulsen *et al.* (1997). A comprehensive discussion of the state of the art in micro-macro simulation techniques can be found in the recent review article by Keunings (2004).

The major advantage of the micro-macro simulation technique is that one can include all the relevant physics at the microscopic scale without the need for any closure approximations. In this context, Bajaj *et al.* (2006) in their recent computation of the slot coating of viscoelastic fluids using a micro-macro simulation algorithm, have shown the significant influence on the predicted values of a number of different properties caused by the inclusion of fluctuating hydrodynamic interactions and finite extensibility in a dumbbell model. It is also worth noting that the issue of the inability of closure approximations to distinguish between *true* and *frozen* steady states does not arise with micro-macro simulations.

Our discussion of nonlinear phenomena at the microscopic scale has clearly indicated that it important to account for the large number of degrees of freedom in a polymer molecule in order to accurately capture all the aspects of the observed behaviour of polymer solutions. Currently, multiscale simulation techniques based on the micro-macro approach are largely confined to dumbbell models, with a single degree of freedom. The extension of these algorithms to bead-spring chain models with many beads represents a major computational hurdle. Thus, although nonlinear microscopic phenomenon can in principle be incorporated directly into the computational algorithm, CPU time considerations have so far prevented a thorough examination of the role of these phenomena in complex flows. Overcoming this problem will make multiscale simulation algorithms a powerful tool in computational rheology in the future.

## 7. Discussion and Conclusions

The key points that have arisen so far from the discussion of the current situation in the pursuit of *micro* and *macro* in complex fluid mechanics can be summarized as follows:

1. The computation of complex fluid flows in the macroscopic cycle has focussed largely on solving benchmark flow problems, in order to understand and tame the high Weissenberg number problem. While increasingly sophisticated numerical algorithms have been developed over the years, numerical simulations still break down for relatively small values of *Wi*. In the case of flow around a cylinder confined between two flat plates, it has been shown that a coil-stretch transition in the wake of the cylinder is responsible for the break down of computations in dilute Oldroyd-B fluids. The unbounded stretching of the Hookean spring that underlies the Oldroyd-B model might also be the source of the HWNP in other benchmark flows.

2. Recent studies of steady flows with an interior stagnation point, and steady stagnation point flows away from a wall, suggest that the mathematical structure of the upper convected Maxwell, Oldroyd-B and FENE-P models can be expected to lead to singularities in the viscoelastic stresses and their gradients with increasing *Wi*. The existence of singular behaviour might be the typical feature of solutions for all constitutive equations which include stress advection and stress relaxation, but do not incorporate stress diffusion.

3. Complex flow situations in which polymer molecules stretch to a contour length that is comparable to the mesh size in finite element simulations, and even to the characteristic dimension of the flow, call into question the assumption of homogenous flow fields with negligible variation on the length scale of individual molecules, commonly made in kinetic theory based constitutive models.

4. It is crucial to incorporate the finite extensibility of polymer chains, excluded volume interactions between segments of a chain, and solvent mediated hydrodynamic interactions in order to capture all the rich diversity of behaviour exhibited by dilute polymer solutions.

5. By using a successive fine-graining procedure, it is possible to avoid the arbitrary specification of parameters in bead-spring chain models, and to obtain, with the help of BD simulations, nearly quantitative agreement with experimental observations in homogeneous flows of a range of different material properties, both at the microscopic and the macroscopic scales.

6. Constitutive equations that reflect the complex physics that is present at the microscopic scale can be developed with the help of closure approximations. The accuracy of these approximations, for some of the microscopic phenomena, have been tested against exact BD simulations, and have been shown to be in good qualitative agreement, and in many cases, even quantitatively accurate.

7. The only constitutive equations based on closure approximations that are currently widely used in the computation of complex flows are those that account for the finite extensibility of polymer chains. Even though constitutive equations that account for other complex microscopic phenomenon such as EV and HI have been around for some years, they have not been used so far for computing complex flows.

8. An alternative approach to complex fluid mechanics can be developed through the use of micro-macro simulations in which nonlinear microscopic physics can be incorporated into the description without the invocation of closure approximations. However, computational time limitations arise for simulations of large bead-spring chains.

Clearly, there are a large number of challenges which must to be tackled before we can successfully compute complex flows of dilute polymer solutions. While signif-

icant progress has been made in achieving convergence of theory with experiment in the microscopic cycle, there are many issues that remain to be resolved in the macroscopic cycle. A mere extension of the capacity of constitutive equations to account for HI and EV will not solve the HWNP. On the other hand, not accounting for these phenomenon will surely lead to poor predictions of experimental observations. There is evidently a need to develop kinetic theory based constitutive models for non-homogeneous flows and to adopt them in complex flow simulations. Further, constitutive equations that account for stress diffusion are necessary to alleviate the development of large stresses and stress boundary layers. A mechanism for accounting for stress diffusion at the microscopic scale would be to allow for centre-of-mass motion across streamlines. The presence of non-homogenous flow fields would also give rise to centre-of-mass motion across streamlines (Bhave *et al*., 1991). Recently, in this context, Schieber (2006) has proposed a generalized Brownian configuration fields method that accounts for centre-of-mass diffusion in the bulk flow, but which is not valid in the vicinity of walls. To our knowledge, this algorithm has not yet been applied to the solution of a complex flow problem. In the context of microfluidic flows, Hernández-Ortiz *et al.* (2007) have recently developed an algorithm for efficient simulation of hydrodynamic interactions between polymer segments in a confined geometry, and have applied it to examining the concentration distributions of polymers in slits and grooved channels (Hernández-Ortiz *et al*., 2008). The larger problem of computing complex flows in complex geometries of general industrial relevance remains a challenging goal that will provide fruitful research opportunities for years to come.

## References


Bajaj, M., P. P. Bhat, J. R. Prakash and M. Pasquali, 2006, "Multiscale simulation of viscoelastic free surface flows," *J. Non-Newtonian Fluid Mech.* **140**, 87-107.

Bajaj, M., M. Pasquali and J. R. Prakash, 2008, "Coil-stretch transition and the breakdown of computations for viscoelastic fluid flow around a confined cylinder," *J. Rheol*. **52**, 197-223.

Becherer, P., A. N. Morozov and W. van Saarloos, 2008, "Scaling of singular structures in extensional flow of dilute polymer solutions," *J. Non-Newtonian Fluid Mech.* **153**, 183-190.

Becherer, P., W. van Saarloos and A. N. Morozov, 2009, "Stress singularities and the formation of birefringent strands in stagnation flows of dilute polymer solutions," *J. Non-Newtonian Fluid Mech.* **157**, 126-132.

Beck, V. A. and E. S. G. Shaqfeh, 2006, "Ergodocity breaking and conformational hysteresis in the dynamics of a polymer thethered at a surface stagnation point," *J. Chem. Phys.* **124**, 094902.

Bhave, A. V., R. C. Armstrong and R. A. Brown, 1991, "Kinetic theory and rheology of dilute, nonhomogeneous polymer solutions," *J. Chem. Phys.* **95**, 2988-3000.

Bird, R. B., R. C. Armstrong and O. Hassager, 1987a, *Dynamics of Polymeric Liquids - Volume 1: Fluid Mechanics*, John Wiley, New York, 2nd edn..

Bird, R. B., C. F. Curtiss, R. C. Armstrong and O. Hassager, 1987b, *Dynamics of Polymeric Liquids - Volume 2: Kinetic Theory*, John Wiley, New York, 2nd edn..

Bird, R. B., P. J. Dotson and N. L. Johnson, 1980, "Polymer solution rheology based on a finitely extensible bead-spring chain model," *J. Non-Newtonian Fluid Mech.* **7**, 213-235.

Bird, R. B. and H. C. Öttinger, 1992, "Transport properties of polymeric liquids," *Ann. Rev. Phys. Chem.* **43**, 371-406.

Boger, D. V., 1996, "Viscoelastic fluid mechanics: interaction between prediction and experiment," *Experimental Thermal and Fluid Science* **12**, 234-243.

Chilcott, M. D. and J. M. Rallison, 1988, "Creeping flow of dilute polymer solutions past cylinders and spheres," *J. Non-Newtonian Fluid Mech.* **29**, 381-432.

Clasen, C., J. P. Plog, W.-M. Kulicke, M. Owens, C. Macosko, L. E. Scriven, M. Verani and G. H. McKinley, 2006, "How dilute are dilute solutions in extensional flows?" *J. Rheol.* **50**, 849-881.

Clasen, C., M. Verani, J. P. Plog, G. H. McKinley and W.-M. Kulicke, 2004, "Effects of polymer concentration and molecular weight on the dynamics of visco-elasto-capillary breakup," in *Proceedings of the XIVth International Congress on Rheology*, pp. PS22-1, Seoul, Korea.

Darinskii, A. A. and M. G. Saphiannikova, 1994, "Kinetics of polymer chains in elongational flow," *J. Non-Crystall. Solids* **172**, 932-934.

De Gennes, P. G., 1974, "Coil-stretch transition of dilute flexible polymers under ultrahigh velocity gradients," *J. Chem. Phys.* **60**, 5030-5042.

De Gennes, P.-G., 1979, *Scaling Concepts in Polymer Physics*, Cornell University Press.

Des Cloizeaux, J. and G. Jannink, 1990, *Polymers in Solution, Their Modeling and Structure*, Oxford Science Publishers.

Doi, M. and S. F. Edwards, 1986, *The Theory of Polymer Dynamics*, Oxford University Press, New York.

Duggal, R., P. Sunthar, J. R. Prakash and M. Pasquali, 2008, "Multiscale simulation of dilute DNA in a roll-knife coating flow," *J. Rheol.* **52**, 1405-1425.

Entov, V. M. and E. J. Hinch, 1997, "Effect of a spectrum of relaxation times on the capillary thinning of a filament of elastic liquid," *J. Non-Newtonian Fluid Mech.* **72**, 31-53.

Fan, X. J., R. B. Bird and M. Renardy, 1978, "A finitely extensible bead-spring chain model for dilute polymer solutions," *J. Non-Newtonian Fluid Mech.* **69**, 1352-1360.

Fattal, R. and R. Kupferman, 2004, "Constitutive laws for the matrix-logarithm of the conformation tensor," *J. Non-Newtonian Fluid Mech.* **124**, 281-285.

François, N., Y. Amarouchene, B. Lounis and H. Kellay, 2009, "Polymer conformations and hysteretic stresses in nonstationary flows of polymer solutions," *Europhys. Lett.* **86**, 34002.

François, N., D. Lasne, Y. Amarouchene, B. Lounis and H. Kellay, 2008, "Drag enhancement with polymers," *Physical Review Letters* **100**, 018302.

Gupta, R. K., D. A. Nguyen and T. Sridhar, 2000, "Extensional viscosity of dilute polystyrene solutions: Effect of concentration and molecular weight," *Phys. Fluids* **12**, 1296-1318.

Hernández-Ortiz, J., J. de Pablo and M. Graham, 2007, "Fast computation of many-particle hydrodynamic and electrostatic interactions in a confined geometry," *Physical Review Letters* **98**, 140602.

Hernández-Ortiz, J., H. Ma, J. de Pablo and M. Graham, 2008, "Concentration distributions during flow of confined flowing polymer solutions at finite concentration: slit and grooved channel," *Korea-Australia Rheology Journal* **20**, 143-152.

Hinch, E. J., 1974, "Mechanical models of dilute polymer solutions for strong flows with large polymer deformations," *in Proc. Symp. Polym. Lubrification* **233**, 241.

Hsieh, C.-C., L. Li and R. G. Larson, 2003, "Modeling hydrodynamic interaction in Brownian dynamics: Simulations of extensional flows of dilute solutions of DNA and polystyrene," *J. Non-Newtonian Fluid Mech.* **113**, 147-191.

Hsieh, C.-C., L. Li and R. G. Larson, 2005, "Prediction of coil-stretch hysteresis for dilute polystyrene molecules in extensional flow," *J. Rheol.* **49**, 1081-1089.

Hulsen, M. A., R. Fattal and R. Kupferman, 2005, "Flow of viscoelastic fuids past a cylinder at high Weissenberg number: Stabilized simulations using matrix logarithms," *J. Non-Newtonian Fluid Mech.* **127**, 27-39.

Hulsen, M. A., A. P. G. van Heel and B. H. A. A. van den Brule, 1997, "Simulation of viscoelastic flows using Brownian configuration fields," *J. Non-Newtonian Fluid Mech.* **70**, 79-101.

Jendrejack, R. M., J. J. de Pablo and M. D. Graham, 2002, "Stochastic simulations of DNA in flow: Dynamics and the effects of hydrodynamic interactions," *J. Chem. Phys.* **116**, 7752-7759.

Keunings, R., 2000, "A survey of computational rheology," in *Proc. XIIIth Int. Congr. on Rheology*, eds. D. M. Binding, N. E. Hudson, J. Mewis, J.-M. Piau, C. J. S. Petrie, P. Townsend, M. H. Wagner and K. Walters, vol. 1, pp. 7-14, Cambridge, UK.

Keunings, R., 2004, "Micro-macro methods for the multiscale simulation of viscoelastic flow using molecular models of kinetic theory," in *Rheology Reviews 2004*, eds. D. M. Binding and K. Walters, pp. 67-98, British Society of Rheology, Aberystwyth, Wales.

Kirkwood, J. G. and J. Riseman, 1948, "The intrinsic viscosities and diffusion constants of flexible macromolecules in solution," *J. Chem. Phys.* **16**, 565-573.

Kröger, M., A. Alba-Pérez, M. Laso and H. C. Öttinger, 2000, "Variance reduced Brownian simulation of a bead-spring chain under steady shear flow considering hydrodynamic interaction effects," *J. Chem. Phys.* **113**, 4767-4773.

Kumar, K. S. and J. R. Prakash, 2003, "Equilibrium swelling and universal ratios in dilute polymer solutions: Exact Brownian dynamics simulations for a delta function excluded volume potential," *Macromolecules* **36**, 7842-7856.

Larson, R. G., 2004, "The rheology of dilute solutions of flexible polymers: Progress and problems," *J. Rheol*. **49**, 1-70.

Larson, R. G., H. Hu, D. E. Smith and S. Chu, 1999, "Brownian dynamics simulations of a DNA molecule in an extensional flow field," *J. Rheol.* **43**, 267-304.

Laso, M. and H. Ottinger, 1993, "Calculation of viscoelastic flow using moleculat models: the CON54 NFFESSIT approach," *J. Non Newtonian Fluid Mech.* **47**, 1-20.

Li, L., R. G. Larson and T. Sridhar, 2000, "Brownian dynamics simulations of dilute polystyrene solutions," *J. Rheol.* **44**, 291-322.

Liu, S., B. Ashok and M. Muthukumar, 2004, "Brownian dynamics simulations of bead-rod-chain in simple shear flow and elongational flow," *Polymer* **45**, 1383-1389.

Marko, J. F. and E. D. Siggia, 1995, "Stretching DNA," *Macromolecules* **28**, 8759-8770.

McKinley, G. H. and T. Sridhar, 2002, "Filament-stretching rheolmetry of complex fluids," *Annu. Rev. Fluid Mech.* **34**, 375-415.

Öttinger, H. C., 1987, "Generalized Zimm model for dilute polymer solutions under theta conditions," *J. Chem. Phys.* **86**, 3731-3749.

Öttinger, H. C., 1989, "Gaussian approximation for Rouse chains with hydrodynamic interaction," *J. Chem. Phys.* **90**, 463-473.

Öttinger, H. C., 1995, "Letter to the editor: Mesh refinement limits in viscoelastic flow calculations?" *J. Rheol.* **39**, 987-982.

Öttinger, H. C., 1996, *Stochastic Processes in Polymeric Fluids*, Springer-Verlag.

Owens, R. G. and T. N. Phillips, 2002, *Computational Rheology, Imperial College Press*, London, 1st edn..

Pasquali, M. and L. E. Scriven, 2004, "Theoretical modelling of microstructured liquids: A simple thermodynamic approach," *J. Non-Newtonian Fluid Mech.* **120**, 101-135.

Pham, T. T., P. Sunthar and J. R. Prakash, 2008, "An alternative to the bead-rod model: Bead-spring chains with successive fine graining," *J. Non-Newtonian Fluid Mech.* **149**, 9-19.

Prabhakar, R. and J. R. Prakash, 2002a, "Behavior of FENE dumbbells with excluded volume in shear and extensional flows (paper 428)," in *9th APCChE Congress and CHEMECA, Christchurch, New Zealand 29 Sept-3 Oct*.

Prabhakar, R. and J. R. Prakash, 2002b, "Viscometric functions for Hookean dumbbells with excluded volume and hydrodynamic interaction," *J. Rheol.* **46**, 1191-1220.

Prabhakar, R. and J. R. Prakash, 2004, "Multiplicative separation of the influences of excluded volume, hydrodynamic interactions and finite extensibility on the rheological properties of dilute polymer solutions," *J. Non-Newtonian Fluid Mech.* **116**, 163-182.

Prabhakar, R. and J. R. Prakash, 2006, "Gaussian approximation for finitely extensible bead-spring chains with hydrodynamic interaction," *J. Rheol.* **50**, 561-593.

Prabhakar, R., J. R. Prakash and T. Sridhar, 2004, "A successive fine-graining scheme for predicting the rheological properties of dilute polymer solutions," *J. Rheol.* **48**, 1251-1278.

Prabhakar, R., J. R. Prakash and T. Sridhar, 2006, "Effect of configuration-dependent intramolecular hydrodynamic interaction on elastocapillary thinning and breakup of filaments of dilute polymer solutions," *J. Rheol.* **50**, 925-947.

Prakash, J. R., 1999, "The kinetic theory of dilute solutions of flexible polymers: Hydrodynamic interaction," in *Advances in flow and rheology of non-Newtonian fluids*, eds. D. A. Siginer, D. D. Kee and R. P. Chhabra, pp. 467-517, Rheology Series, Amsterdam, Elsevier Science.

Prakash, J. R., 2001, "Rouse chains with excluded volume inter-

actions: Linear viscoelasticity," *Macromolecules* **34**, 3396-3411.

Prakash, J. R., 2002, "Rouse chains with excluded volume interactions in steady simple shear flow," *J. Rheol.* **46**, 1353-1380.

Prakash, J. R. and H. C. Öttinger, 1999, "Viscometric functions for a dilute solution of polymers in a good solvent," *Macromolecules* **32**, 2028-2043.

Rallison, J. M. and E. J. Hinch, 1988, "Do we understand the physics in the constitutive equation?" *J. Non-Newtonian Fluid Mech.* **29**, 37-55.

Renardy, M., 2006, "A comment on smoothness of viscoelastic stresses," *J. Non-Newtonian Fluid Mech.* **138**, 204-205.

Rotne, J. and S. Prager, 1969, "Variational treatment of hydrodynamic interaction in polymers," *J. Chem. Phys.* **50**, 4831-4837.

Rouse, P. E., 1953, "A theory of the linear viscoelastic properties of dilute polymer solutions of coiling polymers," *J. Chem. Phys.* **21**, 1272-1280.

Schäfer, L., 1999, *Excluded Volume Effects in Polymer Solutions*, Springer-Verlag, Berlin.

Schieber, J. D., 2006, "Generalized Brownian configuration fields for Fokker-Planck equations includingcenter-of-mass diffusion," *J. of Non-Newtonian Fluid Mech.* **135**, 179-181.

Schroeder, C. M., H. P. Babcock, E. S. G. Shaqfeh and S. Chu, 2003, "Observation of polymer conformation hysteresis in extensional flow," *Science* **301**, 1515-1519.

Schroeder, C. M., E. S. G. Shaqfeh and S. Chu, 2004, "Effect of hydrodynamic interactions on DNA dynamics in extensional flow: Simulation and single molecule experiment," *Macromolecules* **37**, 9242-9256.

Shaqfeh, E. S. G., 2005, "The dynamics of single-molecule DNA in flows," *J. Non-Newtonian Fluid Mech.* **130**, 1-28.

Sridhar, T., D. A. Nguyen, R. Prabhakar and J. R. Prakash, 2007, "Rheological observation of glassy dynamics of dilute polymer solutions near the coil-stretch transition in elongational flows," *Physical Review Letters* **98**, 167801.

Sunthar, P. and J. R. Prakash, 2005, "Parameter-free prediction of DNA conformations in elongational flow by Successive Fine Graining," *Macromolecules* **38**, 617-640.

Sunthar, P. and J. R. Prakash, 2006, "Dynamic scaling in dilute polymer solutions: The importance of dynamic correlations," *Europhys. Lett.* **75**, 77-83.

Tanner, R., 1975, "Stresses in dilute solutions of bead-nonlinear-spring macromolecules. III. Friction coefficient varying with dumbbell extension," *J. Rheol.* **19**, 557-582.

Tirtaatmadja, V. and T. Sridhar, 1993, "A filament stretching device for measurement of extensional viscosity," *J. Rheol.* **37**, 1081-1102.

Wapperom, P. and M. Renardy, 2005, "Numerical prediction of the boundary layers in the flow around a cylinder using a fixed velocity field," *J. Non-Newtonian Fluid Mech.* **125**, 35-48.

Warner, H. R., 1972, "Kinetic theory and rheology of dilute suspensions of finitely extensible dumbbells," *Ind. Eng. Chem. Fundam.* **11**, 379-387.

Wedgewood, L. E., 1989, "A Gaussian closure of the second-moment equation for a Hookean dumbbell with hydrodynamic interaction," *J. Non-Newtonian Fluid Mech.* **31**, 127-142.

Wedgewood, L. E. and H. C. Öttinger, 1988, "A model of dilute polymer solutions with hydrodynamic interaction and finite extensibility. II. Shear flows," *J. Non-Newtonian Fluid Mech.* **27**, 245-264.

Wiest, J. M., L. E. Wedgewood and R. B. Bird, 1989, "On coil-stretch transitions in dilute polymer solutions," *J. Chem. Phys.* **90**, 587-594.

Yamakawa, H., 1971, *Modern Theory of Polymer Solutions*, Harper and Row, New York.

Zimm, B. H., 1956, "Dynamics of polymer molecules in dilute solution: Viscoelasticity, flow birefringence and dielectric loss," *J. Chem. Phys.* **24**, 269-278.

Zimm, B. H., 1980, "Chain molecule hydrodynamics by the Monte-Carlo method and the validity of the Kirkwood-Riseman approximation," *Macromolecules* **13**, 592-602.

Zylka, W., 1991, "Gaussian approximation and Brownian dynamics simulations for Rouse chains with hydrodynamic interaction undergoing simple shear flow," *J. Chem. Phys.* **94**, 4628-4636.